Journal of Molecular Structure 1285 (2023) 135521

Contents lists available at ScienceDirect

Journal of Molecular Structure

journal homepage: www.elsevier.com/locate/molstr

Identification of some novel amide conjugates as potent and gastric sparing anti-inflammatory agents: *In vitro, in vivo, in silico* studies and drug safety evaluation

Necla Kulabaş[a], İrem Set[b], Göknur Aktay[c], Şule Gürsoy[d], Özkan Danış[e], Ayşe Ogan[e], Safiye Sağ Erdem[e], Pınar Erzincan[e], Sinem Helvacıoğlu[f], Muhammed Hamitoğlu[f], İlkay Küçükgüzel[a,*]

[a] Department of Pharmaceutical Chemistry, Faculty of Pharmacy, Marmara University, Maltepe 34854, İstanbul, Turkey
[b] Institute of Health Sciences, Marmara University, Kartal 34865, İstanbul, Turkey
[c] Department of Pharmacology, Faculty of Pharmacy, İnönü University, 44280, Malatya, Turkey
[d] Department of Biochemistry, Faculty of Pharmacy, Erzincan Binali Yıldırım University, 24002, Erzincan, Turkey
[e] Department of Chemistry, Faculty of Science, Marmara University, 34722, İstanbul, Turkey
[f] Department of Toxicology, Faculty of Pharmacy, Yeditepe University, 34755 Istanbul, Turkey

ARTICLE INFO

Article history:
Received 29 October 2022
Revised 30 March 2023
Accepted 5 April 2023
Available online 5 April 2023

Keywords:
Analgesic effect
Anti-inflammatory effect
Molecular modeling
Non-steroid anti-inflammatory drugs
Cyclooxygenase (COX) inhibitors

ABSTRACT

Today, usage of NSAIDs (nonsteroidal anti-inflammatory drugs) is very common. However, it has been proven by many studies that NSAIDs with free carboxylic acid group damage the GI (gastrointestinal) system. Our aim was to mask the acidic groups of NSAIDs to prevent or reduce their side effects while preserving their pharmacological effects. In this study, new amide derivatives of known NSAIDs, compounds **11**–**20**, were synthesized to investigate their analgesic and anti-inflammatory effects using *in vivo* models. While compound **11** showed the most remarkable anti-inflammatory activity by 60.9% inhibition value at 200 mg/kg dose, compounds **11, 12, 15** and **18** had almost the same analgesic activity to that of acetylsalicylic acid (100 mg/kg) and flurbiprofen (100 mg/kg). In addition, all test compounds used at high dose (200 mg/kg, p.o) did not show any acute toxicity. COX-1 and COX-2 inhibition properties of all compounds were measured by biochemical methods and the interaction of the most active compounds with COX enzymes is elucidated by computer-assisted virtual screening methods. It was determined by *in vitro* enzyme inhibition studies that compound **11** and **13**, synthesized from selective COX-1 inhibitors dexketoprofen and flurbiprofen, are selective COX-2 inhibitors. Moreover, compounds **11**–**13** were found to be non-mutagenic according to the mutagenicity assay using *Salmonella TA98* and *TA100* strains with and without metabolic activation. Finally, the prediction of ADMET profile and drug-likeness properties of compounds **11**–**20** were examined and the obtained results were evaluated.

1. Introduction

After the discovery of Aspirin, the first NSAID effective drug, in 1897, many NSAIDs with different anti-inflammatory and analgesic effect profiles and pharmacodynamic properties have been widely used in the treatment of acute and chronic pain. It has been reported in the literature that this broad class of drugs exert their anti-inflammatory effects by inhibiting prostaglandin biosynthesis. However, the use of these drugs is also associated with a broad spectrum of side effects, that occur with the inhibition of the synthesis of prostaglandins (PG), which is responsible for physiological homeostasis [1].

NSAIDs are a class of drugs that target the cyclooxygenase enzyme in the treatment of pain and inflammation, and prevent prostaglandin synthesis by non-selective inhibition of cyclooxygenases (COX). There are two known isoforms of cyclooxygenases, COX-1 and COX-2. The vasodilating properties of prostacyclins PGE2 and PGI2 produced by the COX-1 enzyme contribute to an increase in mucus secretion in the stomach, as well as a decrease in acidity and pepsin content, thus protecting the integrity of the gastric mucosa. In the kidneys, these prostacyclins stimulate vasoconstriction and increase blood flow in response to factors that contribute to the glomerular filtration rate in case of volume depletion. It has been reported that, long-term use of COX-1 inhibitors

* Corresponding author.
E-mail address: ikucukguzel@marmara.edu.tr (İ. Küçükgüzel).

https://doi.org/10.1016/j.molstruc.2023.135521
0022-2860/

could give rise to the irritation of the gastrointestinal tract, and organ damage such as liver and kidney failure [2]. Therefore, long-term inhibition of COX-1 is thought to be the mechanism of gastric ulcer formation induced by NSAIDs [3,4].

The discovery of inducible COX-2 at sites of inflammation has led to the development of novel selective inhibitors to reduce GI side effects caused by conventional NSAIDs. Since selective COX-2 inhibitors promise to provide a strong anti-inflammatory and analgesic effect without the side effects caused by non-selective COX inhibitors, it has been suggested that selective COX-2 inhibitors might be safer NSAIDs. Thus, selective COX-2 inhibitors that are currently used in clinical practice have been developed [5]. However, long-term use of these agents has demonstrated some potential limitations, including ulcer exacerbation, delayed GI ulcer healing, renal toxicity, and cardiovascular side effects in high-risk patients [6].

The clinical studies have shown an association between the use of selective COX-2 inhibitors, such as rofecoxib and celecoxib, and an increased incidence of stroke and myocardial infarction. These adverse effects were attributed to COX-2 inhibition related suppression of prostacyclin levels which have a vasodilating effect due to responsible for inhibition of platelet aggregation. These data indicate that the safety of these agents in long-term use is questionable, and celecoxib is still in therapeutic use today, with less cardiovascular toxicity than other coccib derivatives, while rofecoxib and valdecoxib have been withdrawn from the market [7–11].

Many similar studies showing the importance of COX-2 inhibitors in cancer chemotherapy [12] and neurological disorders such as Alzheimer's [13] and Parkinson's diseases show that the development of COX-2 inhibitors remains attractive [8,14,15].

Gastrointestinal toxicity of NSAIDs is thought to be due to the irritation of their acidic groups in the gastrointestinal tract and regional inhibition of prostaglandin synthesis [16,17]. Most of the strategies reported in the literature are to identify new targets associated with inflammation, to improve the therapeutic efficacy and tolerability of NSAIDs, or to modify NSAIDs with groups that protect the GI tract [18].

In order to minimize the side effects of this group of drugs, the preparation of prodrugs by masking acidic groups has been one of the most preferred methods. When designing prodrugs of NSAIDs to reduce side effects, combining them with another drug or attaching a chemical group that can modify their pharmacokinetic properties are the most preferred approaches. Interest to ester and amide prodrugs prepared from NSAID drugs have increased in recent studies; because they are substrates of esterase and amidase enzymes *in vivo* and have suitable *in vitro* chemical stability, and can be formulated with sufficient shelf life. Higher solubility, improved bioavailability and lower side-effect profile are targeted in new molecules designed for this purpose. In addition, since the metabolic profiles of NSAIDs used in the clinic are known, the synthesis of derivatives that can release the parent drug in living organisms will be more rational [19–21].

In the light of these findings, we aimed to convert some NSAID molecules containing carboxylic acid groups into their amphiphilic amide derivatives, compounds **11**–**20**, by combining them with tris(hydroxymethyl)aminomethane (TRIS). The hydrolysis potentials of compounds **11**–**13** in simulated gastric fluid (pH 1.2) and intestinal fluid (pH 6.8) have been previously reported [22]. Hydrolysis and degradation studies for compounds **11**–**13** showed that these new amide derivatives were not hydrolysed even after 24 h in both conditions. However, the compounds were found to be N-protonated in acidic medium (pH 1.2) [23]. At the end of these studies, it was concluded that the synthesized derivatives were more stable than related starting materials. The scope of the study was to reveal the pharmacological profiles of these new NSAID candidates, with high analgesic and anti-inflammatory activities and low ulcer-formation potential and oxidative stress parameters, on *in vivo* studies. In addition, it was among our goals to examine the COXs enzyme inhibitory potentials of the synthesized amide derivatives, to evaluate the COX-1/COX-2 selectivity. The results of computer-aided molecular modeling studies provided insight into the binding mechanisms of these compounds and supported the enzyme assay results. Prediction of molecular descriptors and ADMET profiles revealed drug-likeness properties of the synthesized compounds.

2. Results and discussion

2.1. Chemistry

The novel amide derivatives of known NSAIDs, compounds **11**–**20,** were synthesized using reaction protocol outlined in Scheme 1. Firstly, ten different NSAIDs carrying free acid groups were converted to their corresponding methyl esters [1–10]. The target compounds [11–20] were obtained as a result of heating related ester derivatives with TRIS in the presence of anhydrous potassium carbonate in DMSO. It was not possible to react NSAIDs containing carboxylic acid groups directly with TRIS using a coupling agent such as DCC, as it gave rise to multiple by-products. This method provided a simple and selective amide formation starting from ester and a nucleophilic amine without the need for expensive coupling agents or protection of alcohol functions.

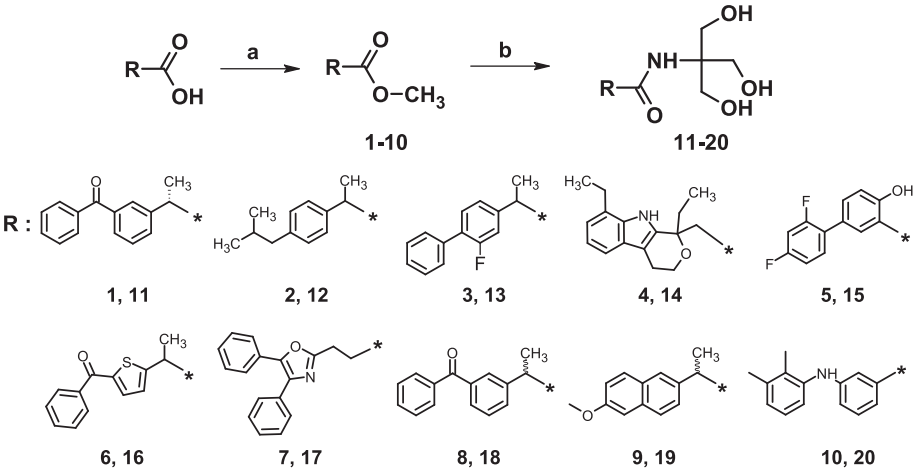

Scheme 1. Synthetic route to compounds **1–20**. Reagents and conditions: ***i.*** d.H_2SO_4, MeOH; ***ii.*** $H_2NC(CH_2OH)_3$, K_2CO_3, DMSO.

All synthesized compounds were checked for purity and identity using TLC and HPLC-UV/DAD analysis. The new amide derivatives **11**–**20** were characterized by their melting points, FTIR, ^{1}H NMR, ^{13}C NMR and mass spectral data, besides elemental analysis. We determined that all spectral data were in agreement with the structures of target compounds. In the IR spectra of compounds **11**–**20**, determination of carbonyl stretching bands at 1620–1647 cm^{-1} instead of the bands at 1702–1740 cm^{-1} clearly proves the formation of amide derivatives. ^{1}H NMR spectra also provided support for the structures of the synthesized compounds **11**–**20** by the detection of N–H resonances of the amide function in the range of 7.14–11.85 ppm, which was a very wide range since many different NSAIDs were used as starting materials. The mentioned spectra of compounds **11**–**20** with all TLC and HPLC data were given in Supplementary Materials.

2.2. Biological activity studies

2.2.1. Analgesic and anti-inflammatory activity

Gastric ulceration risk studies. The compounds, which were screened for anti-inflammatory activity, were further screened for their acute ulcerogenic risk. As a general consideration, all compounds except compounds **14** and **18** were found to be safer as gastric lesion risks at high dose (200 mg/kg, p.o) when compared to indomethacin (INDO) and flurbiprofen (FLU) (Table 1).

Analgesic activity. As seen in Table 1, compounds **11, 12, 15** and **18** had almost the same analgesic activity as acetylsalicylic acid (ASA)(100 mg/kg) and FLU (100 mg/kg). The compounds **13, 17** and **19** nonetheless had a little analgesic activity.

Anti-inflammatory activity. The anti-inflammatory activity of the amide derivatives **11–20** was assessed by their ability to inhibit the paw edema induced by carrageenan in mice and activity was expressed as "mean increase in paw volume±SD" in terms of mm and percentage inhibition (inhibition%) in paw volume by different doses of the compounds [24]. As seen in Table 1, all of the compounds, except compounds **15, 16, 17, 19** and **20**, possessed moderate to very good anti-inflammatory activity at all doses and in any of the measurement intervals. Among the compounds tested, the compounds **11, 12** and **14** showed the most remarkable activity at 200 mg/kg dose (to 60.9% inhibition). However, the compounds **13** and **18** when administered a decreasing dose (50 mg/kg), the activity was found to have increased dramatically. It is well known that an edema produced by carrageenan is a biphasic event and if the inhibition is more effective in the first phase of carrageenan-induced edema, it means that the response is mediated by histamin or serotonin. However, if the inhibition is more effective in the second phase of carrageenan-induced edema, it means that the reply is prostaglandin-mediated [25]. It might be stated that our compounds show their anti-inflammatory activity through the PG-mediated mechanism. In order to enlighten the mechanism clearly, further studies have to be made with serotonin, histamine and PG.

Acute toxicity test. Test compounds administered at the high dose (200 mg/kg, p.o), did not show any acute toxicity. Common side effects such as diarrhea and depression were not recorded.

Lipid peroxidation in tissues. It has been well known that lower ulcerogenic risk of the compounds is combined with a reduced TBARS content in the affected area of the gastrointestinal tract, by products of lipid peroxidation. Therefore, an attempt was made to correlate the decrease in ulcerogenic effect of the compounds with that of lipid peroxidation [26]. The compounds **11** and **12** showed good antioxidant activity compared to other compounds. As seen in Table 2, INDO and FLU showed significant increase in TBARS level. An important finding of the tissue lipid peroxidation results that kidney TBARS levels significantly higher in all groups than control. Therefore, it may be important to investigate the pharmacokinetics of the compounds in future studies.

The results further suggested that their diminished harmful effects on the stomach might be related to their antioxidant properties. The fact that the compounds with low ulcerogenic risk do not cause any increase on stomach lipid peroxidation level leads us to think that the antioxidant properties of these compounds contribute to the anti-inflammatory activities.

GSH and TSH levels. Reduced glutathione (GSH) is the most prevalent non-protein thiol in animal cells and a central component in the antioxidant defense of cells, acts both by detoxifying free oxygen radicals directly. GSH content was similar to control animals in all groups except compounds **13** and **18** in all tissues (Table 2).

2.2.2. In vitro *cyclooxygenase enzymes inhibition*

Ten newly synthesized compounds were evaluated *in vitro* for their COX-1 and COX-2 inhibition ability and selectivity. All assays were performed in triplicates. The inhibitory activity in terms of IC_{50} values in addition to the selectivity index were summarized in Table 3. The obtained results were compared with reference inhibitors, celecoxib, dexketoprofen, flurbiprofen and indomethacin.

The IC_{50} values of celecoxib (potent selective COX-2 inhibitor) on COX-1 and COX-2 were determined to be 16.012 μM and 0.07 μM respectively, with high SI (228.7). The reference standard inhibitors show that we have achieved similar results with the existing literature in this enzyme immunoassay system [27–32]. Compound **20** with an IC_{50} value $>$100 μM for COX-1 and 0.16 μM for COX-2 and selectivity index $>$625, was found to be the most selective COX-2 inhibitor ($\geq$2.7 fold higher than celecoxib). The results showed that all tested compounds were actively inhibited COX-1 with IC_{50} values ranging $<$0.05–16.125 μM except compound **20**. With respect to inhibitory activity on COX-2, all tested compounds except **16**, showed potent COX-2 inhibition with IC_{50} values ranging from $<$0.05–3.66 μM that three of them (compounds **15, 17** and **19**) showed better inhibition than celecoxib. Although dexketoprofen is a selective COX-1 inhibitor, *in vitro* studies showed that, compound **11** synthesized from dexketoprofen is a selective COX-2 inhibitor (SI (COX-1/COX-2): 14.30). A similar finding has been detected that the COX-1/COX-2 selectivity index of compound **13**, which was synthesized from flurbiprofen, increased 150 times in favor of COX-2, with respect to flurbiprofen (Table 3). Though the selectivity of compound **18** synthesized from the racemic ketoprofen changed in the direction of COX-2 (SI (COX-1/COX-2): 3.06), was found lower than compound **11**.

2.2.3. Mutagenicity studies

Genotoxicity testing is a critical component of safety assessment of xenobiotics. It is designed to detect genetic damage such as gene mutations and chromosomal aberration, which may be reflected in tumorigenic or heritable mutation potential of the materials [33]. In this study, we investigated the mutagenicity assay induced by compounds **11, 12** and **13** in the TA98 and TA100 strains with and without metabolic activation. TA98 and TA100 strains were selected for detection of frameshift and base pair substitution mutations, respectively. The positive control showed high frequencies of revertant colonies when compared to negative control ($p < 0.01$) in both investigated strains with and without S9 activation (Tables 4 and 5). The results of the mutagenicity assay showed that none of the tested concentrations of compounds **11, 12** and **13** induced a significant increase in the revertant number of TA98 and TA100 strains, indicating no mutagenicity to the tested strains whether or not incubated with S9.

Table 1
Anti-inflammatory effects of the test compounds against carrageenan-induced hind paw oedema and acetic acid-induced abdominal constriction as writhing reflex tests in mice (n = 4–5).

Compounds	Dose	Ulcer score	Writhing reflex±SD (% inh.) 100 mg/kg	90 min. mean±SD (% inh.)	180 min. mean±SD (% inh.)	270 min. mean±SD (% inh.)	360 min. mean±SD (% inh.)
Control	**100**	0/5	25.0 ± 6.5	55.0 ± 5.2	54.0 ± 4.6	79.0 ± 4.0	89.0 ± 4.4
ASA 200 mg/kg	**50**	3/5	10.0 ± 5.9 ** **(60.0)**				
INDO 10 mg/kg	**200 mg/kg**	3/5	–	41.0 ± 5.0 ** **(25.5)**	39.0 ± 2.9 *** **(27.7)**	44.0 ± 4.8 *** **(44.3)**	41.0 ± 3.3 *** **(53.9)**
FLU 50 mg/kg		4/5	10.1 ± 1.9** **(59.6)**				
11		0/5	4.0 ± 8.9 ** **(84.0)**	65.0 ± 7.1	42.5 ± 3.2 ** **(21.3)**	40.0 ± 5.4 *** **(49.4)**	53.7 ± 4.3 *** **(39.7)**
				52.5 ± 3.2	47.5 ± 4.3	53.7 ± 2.4 *** **(32.0)**	65.0 ± 2.1 *** **(27.0)**
				26.1 ± 5.3 *** **(52.6)**	21.1 ± 7.6 *** **(60.9)**	38.6 ± 7.9 *** **(51.1)**	55.6 ± 9.3 ** **(37.5)**
12		0/5	10.0 ± 9.3 * **(60.0)**	48.7 ± 3.1	36.2 ± 3.1 *** **(33.0)**	40.0 ± 3.6 *** **(49.4)**	68.7 ± 2.4 *** **(22.8)**
				35.0 ± 5.4 *** **(36.4)**	41.2 ± 3.7 * **(23.7)**	57.5 ± 3.2 *** **(27.2)**	67.5 ± 1.4 *** **(24.2)**
				26.1 ± 11.3 ** **(52.6)**	24.2 ± 5.7 *** **(55.2)**	43.9 ± 5.1 *** **(44.3)**	45.9 ± 8.4 *** **(48.4)**
13		0/5	18.0 ± 5.9 **(28.0)**	47.5 ± 5.2	46.2 ± 4.3 *	50.0 ± 3.5 *** **(36.6)**	60.0 ± 4.6 *** **(32.6)**
				36.2 ± 4.3***(34.2)	42.5 ± 4.3 ** **(21.3)**	52.5 ± 3.2 ***(33.5)	58.7 ± 5.5 *** **(34.0)**
				55.0 ± 7.8	36.3 ± 10.4 * **(32.8)**	61.4 ± 12.7 * **(22.3)**	68.9 ± 8.2 * **(22.6)**
14		1/5	26.0 ± 7.8	37.5 ± 3.2 *** **(31.8)**	50.0 ± 3.5	57.5 ± 5.2 *** **(27.2)**	68.7 ± 4.3 *** (22.8)
				37.5 ± 3.2 *** **(31.8)**	32.5 ± 3.2 *** **(39.8)**	46.2 ± 3.2 ***(41.5)	65.0 ± 4.6 *** **(26.9)**
				28.8 ± 5.3 *** **(47.6)**	27.2 ± 6.0 *** **(49.7)**	59.9 ± 7.9 ** (24.0)	68.9 ± 4.6 *** (22.6)
18		3/5	11.6 ± 1.7 **(53.6)	55.4 ± 4.2	42.4 ± 4.3**(21.5)	76.2 ± 5.2	75.4 ± 4.6**
				46.2 ± 7.3	35.0 ± 5.2 ***(35.2)	59.3 ± 7.4***(25)	72.7 ± 6.7**
				68.3 ± 10.6	52.6 ± 8.1	55.9 ± 8.6***(29.2)	68.3 ± 11.2** **(23.2)**
15			10.6 ± 1.8 ** **(57.6)**	–	–	–	–
16			23.9 ± 2.9	–	–	–	–
17			17.7 ± 4.3 **(29.2)**	–	–	–	–
19			17.9 ± 2.4 **(28.4)**	–	–	–	–
20			22.8 ± 3.1	–	–	–	–

Statistical analysis of data;
Data obtained from animal experiments were expressed as means±standard deviation (SD). Statistical differences between the treatment and the control group of animals were evaluated by two-tailed Student's t-test.
* $p<0.05$ (significant).
** $p<0.01$ (very significant).
*** $p<0.001$(extremely significant).

Table 2
Lipid peroxidation (as TBARs, nmol/g wet weight), GSH (µmol/g wet weight) and TSH (µmol/g wet weight) levels in stomach, liver and kidney at 200 mg/kg doses of test compounds.

Compounds	Lipid PeroxidationTBARS			GlutathioneGSH			Total thiol groupsTSH		
	Stomach	Liver	Kidney	Stomach	Liver	Kidney	Stomach	Liver	Kidney
Control	145.0 ± 3.8	282.4 ± 19.2	460.4 ± 15.3	1.5 ± 0.2	5.0 ± 0.2	1.8 ± 0.3	4.5 ± 0.4	19.8 ± 0.5	14.0 ± 0.1
INDO 10 mg/kg	161.0 ± 7.8[a]	373.4 ± 15.1[c]	533.2 ± 10.6[c]	0.8 ± 0.2[b]	3.9 ± 0.6 [b]	0.9 ± 0.2[c]	3.0 ± 0.3[c]	15.4 ± 1.1[c]	11.0 ± 0.5[c]
FLU	161.9 ± 1.1[b]	306.4 ± 18.9	541.6 ± 12.4[c]	0.9 ± 0.1[a]	3.4 ± 0.3 [c]	1.7 ± 0.2	3.5 ± 0.4[a]	16.2 ± 1.1[c]	12.5 ± 0.5[c]
11	139.6 ± 5.2	265.4 ± 16.2	551.4 ± 18.4[c]	1.4 ± 0.3	5.4 ± 0.3	1.7 ± 0.3	3.9 ± 0.3	19.2 ± 0.8	13.2 ± 0.5
12	140.4 ± 6.2	294.6 ± 13.4	549.6 ± 14.2[c]	1.4 ± 0.4	5.6 ± 0.4	1.8 ± 0.3	3.7 ± 0.4	17.9 ± 0.8[a]	13.0 ± 0.3[a]
13	133.8 ± 5.3	238.2 ± 7.7[b]	508.4 ± 15.4[b]	0.9 ± 0.2[a]	4.5 ± 0.3	1.7 ± 0.1	3.9 ± 0.4	17.9 ± 0.9[a]	13.2 ± 0.4
14	155.6 ± 10.2	323.6 ± 16.1[b]	578.8 ± 22.1[c]	1.2 ± 0.2	4.5 ± 0.4	1.5 ± 0.4	3.8 ± 0.5	18.0 ± 0.9[a]	13.0 ± 0.6[a]
18	142.6 ± 8.2	279.7 ± 11.1	505.7 ± 19.4[b]	0.7 ± 0.4[b]	3.3 ± 0.5[c]	1.8 ± 0.3	3.9 ± 0.6	19.7 ± 0.4	13.0 ± 0.5[a]

Statistical analysis of data;
All values are expressed as the mean±SD. The data were analysed by a one-way analysis of variance (ANOVA) followed by a Tukey-Kramer multiple comparisons post hoc test.
[a] $p<0.05$ (significant).
[b] $p<0.01$ (very significant).
[c] $p<0.001$(extremely significant).

Table 3
Inhibitory activity of synthesized amide derivatives against COX-1 and COX-2 enzymes.

Compound	IC_{50} (μM)[a,b]		SI[c]
	COX-1	COX-2	
11	3.400±0.8914	0.238±0.0471	14.30
12	0.658±0.0515	0.449±0.0289	1.50
13	2.286±0.4231	0.1985±0.0162	11.50
14	0.840±0.0743	0.126±0.0171	6.70
15	< 0.05	< 0.05	≈ 1.0
16	16.125±1.9746	>100	< 0.16
17	0.350±0.0252	< 0.05	> 7.0
18	11.230±1.0900	3.669±0.4917	3.06
19	< 0.05	< 0.05	≈ 1.0
20	>100	0.16±0.018	> 625.0
Celecoxib	16.012±1.3476	0.07±0.0043	228.7
Dexketoprofen	0.0005±0.0001	0.0389±0.0058	0.013
Flurbiprofen	0.0015±0.0002	0.0220±0.0018	0.07
Indomethacin	0.0116±0.0025	0.6340±0.0876	0.018

[a] IC_{50} value is the μM concentration required to produce 50% inhibition of the related enzyme. Values are expressed as mean ± SEM ($n = 3$).
[b] IC_{50} values were not determined for compounds showing less than 50% inhibition at concentrations of 100 μM and higher than 50% inhibition at concentrations of 50 nM.
[c] SI, selectivity index is defined as IC_{50} (COX-1)/IC_{50} (COX-2).

Our cytotoxicity results also revealed that toxicity was observed for compound **12** at a concentration of 5000 µg/plate of culture in both strains. The same concentration was found to be toxic in TA100 strain treated with compound **13**. On the other hand, compound **11**, at concentrations up to ≤ 5000 µg/plate did not influence bacterial viability, indicating no toxicity in the tested bacterial strains TA98 and TA100. This observation suggests compound **11** as a safer chemical scaffold compared to compounds **12** and **13**.

2.3. Docking studies

Following the *in vitro* enzyme inhibition assay, the interactions of these compounds with the active site of COX-1 and COX-2 enzymes were investigated by using molecular docking studies. Celecoxib, dexketoprofen and flurbiprofen which were known NSAIDs, were used as reference ligands. The basic structure of COX-1 and COX-2 enzymes are found in many different species and it is known that the amino acid sequences of these enzymes are 60–65% similar in mammalian species. The active sites of both COX isoenzymes are similar and Arg120, Tyr355 and Glu524 residues give rise to a partial constriction at entry into the active site. Eventually, the active site opens into a narrow long hydrophobic channel extending towards a catalytic membrane binding site [15]. Despite all these similarities, as a result of the presence of the Val523 residue in COX-2 instead of the Ile523 residue in COX-1, the 20%

Table 4
Mutagenicity of samples in *Salmonella typhimurium* TA98.

Without S9	Number of revertant/plate		
	Compd **11**	Compd **12**	Compd **13**
Negative control (DMSO)	29.0 ± 7.5		
Positive control	*586.15 ± 42.53		
Dose	**5000**	24.5 ± 4.9	*10.0 ± 2.8	31.5 ± 2.1
(µg/plate)	**1000**	26.0 ± 1.4	21.5 ± 2.1	26.5 ± 3.5
	100	23.0 ± 1.4	28.0 ± 1.4	29.0 ± 2.8
	10	29.5 ± 2.1	27.0 ± 1.4	32.5 ± 2.1
	1	28.5 ± 3.5	24.5 ± 4.9	28.5 ± 7.8
With S9			
Negative control (DMSO)	29.0 ± 4.3		
Positive control	*1046.8 ± 77.1		
Dose	**5000**	26.0 ± 2.8	*7.0 ± 4.2	25.5 ± 3.5
(µg/plate)	**1000**	22.5 ± 3.5	22.0 ± 4.2	28.5 ± 2.1
	100	25.0 ± 2.8	27.0 ± 5.7	29.0 ± 2.8
	10	26.0 ± 4.2	27.5 ± 9.2	24.0 ± 7.1
	1	33.5 ± 0.7	32.0 ± 1.4	27.0 ± 2.8

Dunnett's multiple comparison test was carried out for statistical analysis. NPD (20 µg/plate) was used as positive mutagen without S9. 2-aminofluorene (10 µg/plate) was used as positive mutagen for with S9 experiment.
* $p < 0.05$ *versus* negative control.

Table 5
Mutagenicity of samples in *Salmonella typhimurium* TA100.

Without S9	Number of revertant/plate			
		Compd **11**	Compd **12**	Compd **13**
Negative control (DMSO)	113.2 ± 11.3			
Positive control	*950.0 ± 73.6			
Dose	**5000**	112.5 ± 14.8	*44.0 ± 1.4	*24.5 ± 4.9
(μg/plate)	**1000**	124.5 ± 21.9	125.0 ± 11.3	104.5 ± 6.4
	100	105.0 ± 12.7	117.0 ± 5.7	106.0 ± 12.7
	10	117.5 ± 10.6	128.0 ± 9.9	102.5 ± 7.8
	1	110.0 ± 21.2	113.5 ± 0.7	107.0 ± 12.7
With S9				
Negative control (DMSO)	106.5 ± 16.8			
Positive control	*551.5 ± 46.0			
Dose	**5000**	112.0 ± 14.1	*14.5 ± 0.7	*22.5 ± 10.6
(μg/plate)	**1000**	106.0 ± 8.5	109.0 ± 5.7	100.0 ± 21.2
	100	107.0 ± 2.8	99.5 ± 7.8	108.0 ± 15.6
	10	102.5 ± 17.7	100.5 ± 9.2	96.0 ± 5.7
	1	104.5 ± 10.6	99.0 ± 9.9	119.5 ± 29.0

Dunnett's multiple comparison test was carried out for statistical analysis. SA (1 μg/plate) was used as positive mutagen without S9. 2-aminofluorene (10 μg/plate) was used as positive mutagen with S9 experiment.
* $p < 0.05$ *versus* negative control.

Table 6
Binding energy (kcal/mol) of synthesized compounds and reference ligands.

Compound	ΔG (kcal/mol)				
	COX-1 (Binding Sites)			COX-2	
	Pocket A (Active site)	Pocket B	Gate Pocket of A	Active Site	Selectivity
11	n.b. (S)	−7.7	−7.6	−8.1 (S)	COX-2
12	−6.5 (R)	−7.2	−6.8	−7.3 (R)	COX-2
	n.b. (S)	−7.1	−6.8	−7.3 (S)	COX-2
13	−7.7 (R)	−7.3	−6.3	−6.7 (R)	COX-1
	−7.9 (S)	−7.3	−6.7	−7.1 (S)	COX-1
14	n.b. (R)	n.b.	−6.2	−8.0 (R)	COX-2
	n.b. (S)	n.b.	−6.2	n.b. (S)	COX-1
15	n.b.	−8.3	n.b.	−8.0	similar
16	n.b. (R)	−7.8	−6.4	−7.4 (R)	COX-1
	−6.3 (S)	−7.8	−6.9	−6.9 (S)	COX-1
17	−7.6	−7.4	−7.1	−7.1	COX-1
18	n.b. (R)	−8.1	−7.3	−6.7 (R)	COX-1
	n.b. (S)	−7.7	−7.6	−8.1 (S)	COX-2
19	n.b. (R)	−7.8	−6.6	−7.7 (R)	similar
	n.b. (S)	−7.5	−7.1	−7.3 (S)	similar
20	n.b.	n.b.	−6.6	−8.5	COX-2
Celecoxib	–	–	–	−12.0	COX-2
Dexketoprofen	−9.5	–	–	−9.1	COX-1
Flurbiprofen	−10.0 (S)	–	–	−9.0 (S)	COX-1

n.b.: no binding.

larger binding area observed for COX-2 enzyme is the most important dissimilarity in the active sites of these isoforms [9,34]. These differences have important implications for the selectivity profile of their inhibitors, because of changing the access to the catalytic site of the COX enzymes [5,15,35].

Molecular docking is a very useful and practical structure-based drug design tool which scores the favorable binding modes of a ligand in its biological target. Nevertheless, due to some simplifications and limitations in docking protocols, *in silico* results are not always properly correlated to *in vitro* measurements and may produce false positives [36]. The major limitation in docking algorithms is neglecting the dynamics of the protein such as induced fit effects, allosteric effects and conformational flexibility. Because of the extremely large size of the biological receptors/enzymes, it is still quite challenging to incorporate the full dynamics of the biomacromolecule in docking process [37]. Another simplification is ignoring the solvent water molecules in the target protein. To overcome these problems, molecular dynamics simulations and methods such as MM/PBSA, MM/GBSA [38] can be used for further confirmation for the stability of the docked pose of the enzyme-ligand complex but their high computational cost is a disadvantage.

The results of our docking studies (Table 6) have shown that, in terms of COX-1/COX-2 selectivity, calculated binding energies are in the same direction with the *in vitro* IC_{50} measurements (Table 3), except for compounds **13** and **17**. The differences between results of *in vitro* and *in silico* studies can be due to the limitations mentioned above. Moreover, except compound **11**, the remaining chiral compounds subjected to IC_{50} measurements are in the form of racemic mixtures while the binding energies are calculated for the pure enantiomers, which unfortunately complicates the direct correlation between *in vitro* and *in silico* results.

Calculated binding energies reveal that almost all of these compounds show affinity to COX-2 active site but majority of them do not bind to the the active site pocket of COX-1. This is compatible with the *in vitro* tests in Table 3 displaying COX-2 selectivity in general. On the other hand, according to IC_{50} values, they also exhibit various degrees of COX-1 inhibition which prompted us to

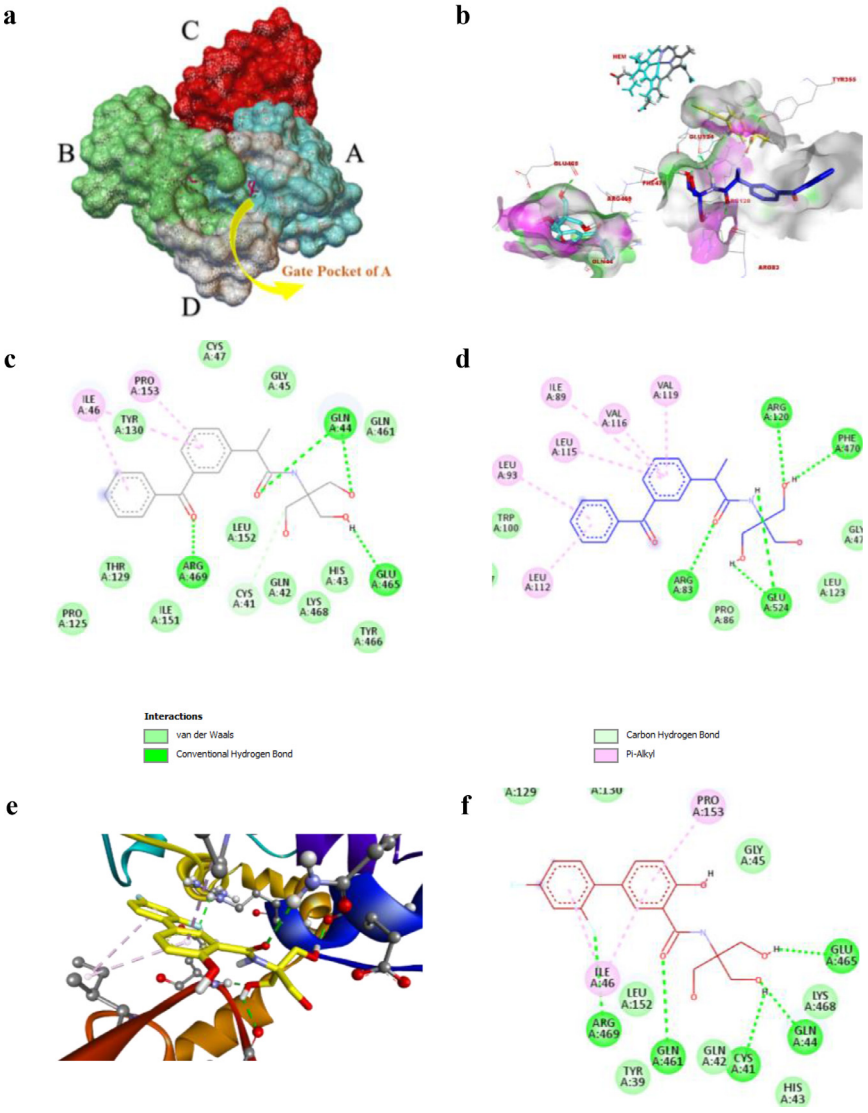

Fig. 1. a) The predicted druggable binding sites of COX-1 according to CavityPlus web server. Pocket A (the cyclooxygenase active site) is blue, Pocket C (peroxidase binding site) is red, pocket B is green and pocket D is gray. b) Alternative bindings of compound **11** with the binding sites of COX-1 enzyme. Co-crystallized ligand (yellow) of COX-1 enzyme (pdb code: 1Q4G) is in the active site (pocket A); one conformation of compound **11** (navy blue) can bind to gate pocket of A while another conformation (turquoise) can bind to the newly identified site (pocket B). c) Interactions between compound **11** and pocket B as 2D diagram. d) Interactions between compound **11** and gate pocket of A as 2D diagram. e) Interactions between compound **15** and pocket B as 3D diagram. f) Interactions between compound **15** and pocket B as 2D diagram. (For interpretation of the references to color in this figure legend, the reader is referred to the web version of this article.)

analyze their docked conformations in COX-1 in more detail. Interestingly, we have noticed that most of them (**11, 12, 14, 15, 16, 18, 19**) bind to different pockets of COX-1 with better affinities, instead of its active site. In order to justify our observation, we explored all the binding pockets of COX-1 employing CavityPlus web server [39–41]. The data generated for all identified binding sites are presented in Table S1 (see in Supplementary Materials). Four of these binding sites which we denoted as A, B, C, D exhibit strong druggability and are shown in Fig. 1a. Among them, pocket A and C are the known cyclooxygenase and peroxidase [42] binding sites of COX-1, respectively. Furthermore, the region where the interaction with Arg120, Tyr355 and Glu-524 residues causing partial constriction at the entry of the active site was detected and denoted as the gate pocket of A.

Compounds **11, 12, 14, 15, 18, 19** and **20** which do not bind to the COX-1 active site in pocket A, have been found to interact with pocket B and/or gate pocket of A with diverse values of binding energies (Table 6). To the best of our knowledge there is no previous study mentioning the pocket B of COX-1, while the binding mode of a ketoprofen derivative with gate pocket of A is also reported by Tziona et al. [43].

According to the *in vivo* studies, compound **11** exhibits the best antiinflammatory activity. Although it is selective to COX-2, it also inhibits COX-1 according to *in vitro* enzyme inhibition assays and molecular docking. Our *in silico* study reveals that its inhibitory activity on COX-1 is the result of less favorable orientation in pocket B (−7.7 kcal/mol) or at the gate pocket of A (−7.6 kcal/mol) relative to its more favorable binding mode in the active site of COX-2 (−8.1 kcal/mol). We present possible binding modes of compound **11** with COX-1 enzyme in Fig. 1b (as 3D diagram), 1c and 1d (as 2D diagrams) to explain its effect on COX-1. In pocket B, it exhibits hydrogen bonds with Gln44, Glu465 and Arg469 residues as well as hydrophobic interactions with Ile46 and Pro153 residues. At the gate pocket of A, hydrogen bond interactions with Arg83, Arg120, Phe470, Glu524 residues and hydrophobic interactions with Ile89, Leu93, Leu112, Leu115, Val116, Val119 residues are observed. An-

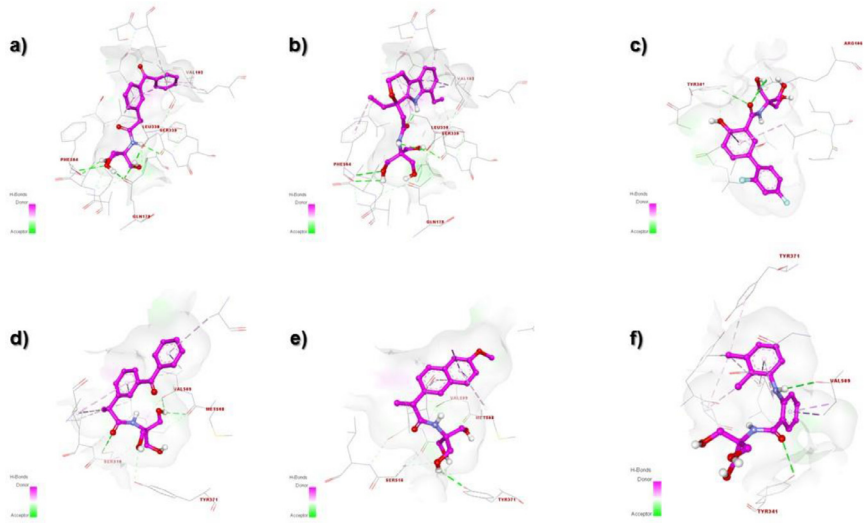

Fig. 2. Binding modes of COX-2 inhibitors in the active site of COX-2. a) Compound **11**; b) compound **14**; c) compound **15**; d) compound **18**; e) compound **19** and f) compound **20**.

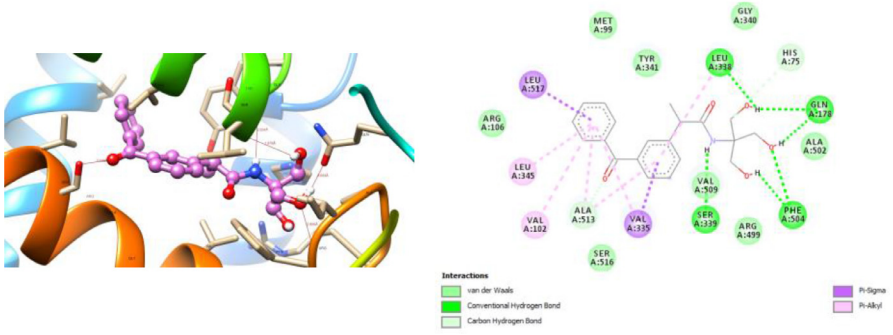

Fig. 3. The interactions of compound **11** with COX-2 active site as 3D and 2D diagrams.

other interesting case is compound **15** which has remarkably high COX-1 enzyme inhibition in *in vitro* experiments but its docked conformations show no binding to the active site pocket A. Instead, it strongly binds to pocket B (−8.3 kcal/mol, Fig. 1e and 1f) of COX-1. It has comparable affinity to the active site of COX-2 (−8.0 kcal/mol) which complies with its nonselective behavior observed in *in vitro* results.

In general, docked conformations of all the synthesized compounds, except *S* isomer of compound **14**, have displayed binding to COX-2 active site while compounds **11, 14, 15, 18, 19, 20** were never attached to the COX-1 active site (pocket A). Therefore, their binding modes in the COX-2 active site are presented in Fig. 2.

Finally, the interactions of compound **11** with COX-2 enzyme are highlighted in 3D and 2-D views in Fig. 3, since it has the highest *in vivo* antiinflammatory activity. The binding energy of compound **11** against COX-2 enzyme has been calculated as $\triangle G$= −8.1 kcal/mol. Various H-bond interactions have been detected between His75, Gln178, Leu338, Ser339, Phe504, Ala513 amino acids and the hydroxyl groups as well as the -NH- proton of the amide structure. Additionally, hydrophobic interactions of both phenyl rings with Val102, Val335, Leu338, Leu345, Ala513 contribute binding of **11** to COX-2.

2.4. Prediction of ADME profile of compounds 11–20

ADMET properties were calculated by using SwissADME calculation software (http://www.swissadme.ch) [44]. SMILES codes of the compounds **11**–**20** were generated from the structures using the ACD/ChemSketch version 12.0 molecular editor. Number of hydrogen bond donors varied from 4 to 5 and the number of hydrogen bond acceptors varied from 4 to 7, while any tested compounds have no more than 10 rotatable bonds (Table S2, see in Supplementary Materials). The bioavailability radars for all the synthesized compounds are given in Fig. 4. The pink-colored zone on the bioavailability radar (SwissADME) presents the optimal range for each property, indicating the drug-likeness of a molecule. All these compounds meet the rules of Lipinski [45], Ghose [46], Veber [47], and Muegge [48].

Estimated intestinal absorption (%ABS) was calculated by:%ABS = 109 − [0.345 × topological polar surface area (TPSA)] according to the method of Zhao et al. [49]. The compounds **11**–**20** were estimated to be highly absorbed in the gastrointestinal tract by 69.05–78.03%ABS values as like the known NSAIDs. Also the newly synthesized compounds **11**–**20** were not BBB permeant, although the NSAIDs except tiaprofenic acid used as starting compounds have BBB permeability (Fig. 4). Compound **18** has been synthesized from racemic ketoprofen, so contains the *R*_isomer of compound **11** as well. Therefore, compound **18** and racemic ketoprofen were not included in the boiled-egg model, as they have the same pharmacokinetic profiles, respectively compound **11** and dexketoprofen.

As a result of *in silico* toxicity predictions, none of the synthesized compounds exhibited mutagenic potential and this finding has been supported by the *in vitro* mutagenicity studies performed for compounds **11, 12, 13** (Fig. S41, see in Supplementary Materials).

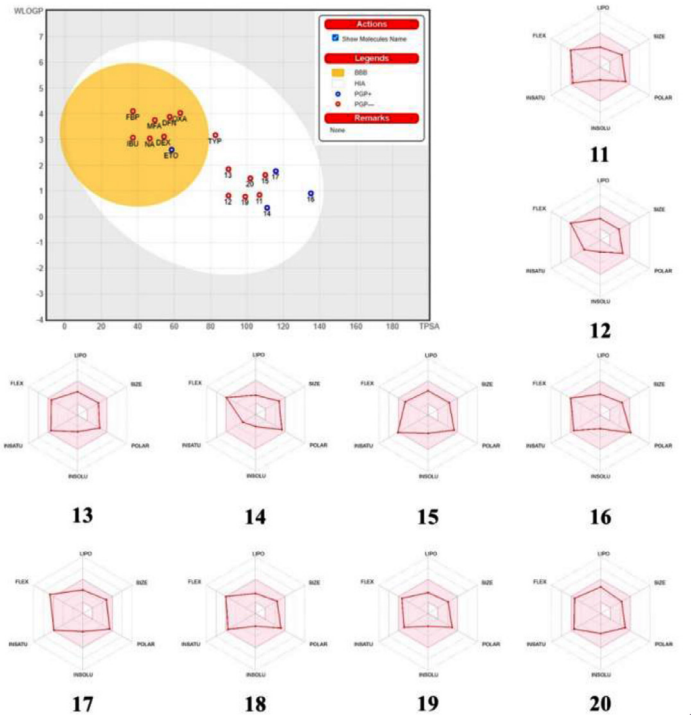

Fig. 4. Boiled-egg diagram for compounds **11**–**20** and their corresponding starting NSAIDs. DEX: Dexketoprofen; IBU: Ibuprofen; FBP: Flurbiprofen; ETO: Etodolac; DFN: Diflunisal; TYP: Tiaprofenic acid; OXA: Oxaprozin; KTP: Ketoprofen; NA: Naproxen; MFA: Mefenamic acid. Bioavailability radars for compounds **11**–**20.** Pink zone—lipophilicity (LIPO) values are within the range −0.7 < XlogP3 < +5.0; molecular weight (SIZE) values are 150 g/mol < MW < 500 g/mol; polarity (POLAR) values are 20 Å2 < TPSA < 130 Å2; insolubility (INSOLU) values are 0 < logS < 6; insaturation (INSATU) values are 0.25 < Fraction Csp3 < 1; flexibility (FLEX) values are 0 < Num. rotatable bonds < 9. 0.

3. Conclusion

In the present study, new amide derivatives were synthesized, in which we covered the free carboxylic acid group of the known NSAIDs to modify their COX-1/COX-2 selectivity and GI side effects. Compounds **11**–**14** and **18** were found to have moderate to very good anti-inflammatory activity at all doses and at any of the specified measuring ranges. Inhibition value up to 60.9% observed for compounds **11, 12** and **14** at 200 mg/kg dose, as well as a marked reduction of anti-inflammatory effect at 50 mg/kg dose for compounds **13** and **18** was noteworthy. The compounds **11, 12, 15** and **18** show similar analgesic effects with acetylsalicylic and flurbiprofen used as references; compounds **13, 17** and **19** were also found to have some analgesic effect. TBARS levels were measured by lipid peroxidation test in tissues for compounds **11**–**14** and compound **18**, which were found to have analgesic effects by *in vivo* studies. While indomethacin and flurbiprofen used as references caused a significant increase in the level of stomach, liver and kidney TBARS, it was determined that all synthesized compounds, especially kidney TBARS levels, were significantly higher than the control group. Therefore, it is important to investigate the pharmacokinetics of the compounds in future studies. It was determined that none of the synthesized amide derivatives showed acute toxicity at high doses (200 mg/kg, p.o) and did not have significant side effects such as diarrhea and depression. The results suggested that the low GI toxicity of the synthesized compounds might be related to their antioxidant properties as well as their resistance to hydrolysis to related NSAIDs [22].

It has been observed by both *in vitro* and *in silico* enzyme inhibition studies that, amide derivatives synthesized have selective COX-2 enzyme inhibition potential, except compounds **15, 16** and **19**. These findings showed us that amide formation altered the selectivity of the NSAIDs towards COX-2. Although the selected three compounds **11**–**13** are not mutagenic in *Salmonella* strains TA98 and TA100, according to OECD guidelines further studies are required using other *Salmonella* strains and also *in vivo*/*in vitro* chromosomal aberration tests before coming to a final conclusion about the mutagenic and genotoxic potential of these compounds. Prediction of ADME profile of compounds **11**–**20** showed that all of these compounds are potential drug candidates with safe and improved pharmacokinetic properties.

4. Materials and methods

4.1. Chemistry

All solvents and reagents were obtained from commercial sources and used without purification. The purity of the compounds was confirmed by the thin-layer chromatography (TLC) performed on Merck silica gel 60 F254 aluminum sheets (Merck, Darmstadt, Germany). The mobile phase was prepared by mixing petroleum ether: ethyl acetate (50:50, v/v). Spots were detected under UV light at λ= 254 nm All melting points (°C, uncorrected) were determined using Schmelzpunktbestimmer SMP II basic model melting point apparatus. Elemental analyses were obtained using Leco CHNS-932 and are consistent with the assigned structures. Infrared spectra were recorded on a Shimadzu FTIR 8400S and data are expressed in wavenumbers $\bar{\nu}$ (cm^{-1}). NMR spectra were recorded on Brüker 300 Mhz Ultrashield TM at 300 MHz for ^{1}H NMR and 75 MHz for ^{13}C NMR (Decoupled), the chemical shifts were expressed in δ (ppm) downfield from tetramethylsilane (TMS) using DMSO-d_6 as solvent. The liquid chromatographic system consists of an Agilent technologies 1100 series instrument equipped with a quaternary solvent delivery system and a model Agilent series G1315 A photodiode array detector. A Rheodyne syringe loading sample injector with a 50 µl sample loop was used for the injection of the analytes. Chromatographic data were

collected and processed using Agilent ChemStation Plus software. The separation was performed at ambient temperature by using a reversed phase. Zorbax-C18 (4.0 × 250 mm, 5 µm particle size) and ACE C18 (4.0 × 100 mm, 5 µm particle size) columns. The separation was performed at ambient temperature by using different mobile phase systems. Solvent delivery was employed at a flow rate of 1 ml min^{-1}. Detection of the analytes was carried out at 210 nm.

*Synthesis of methyl ester derivatives of selected NSAIDs (**1–10**)*

Selected NSAIDs (10 mmol) were dissolved in methanol (40 ml) and added d. H_2SO_4 (1 ml), dropwise. The mixture was heated under reflux for 5 h. Then the solution was cooled and neutralized with 5% $NaHCO_3$ solution. The crude product was drawn into the organic phase by extraction with diethylether. After drying the organic phase with anhydrous sodium sulphate, ether is evaporated to obtain the crude product [50].

*Methyl (2S)-2-(3-benzoylphenyl)propanoate (**1**)*

Yellow liquid (CAS: 81601-91-4), yield 85.3%; TLC Rf: 0.82; HPLC t_R (min): 7.90; IR (cm^{-1}): 1730 (C=O, ester), 1657 (C=O, ketone) [22].

*Methyl 2-[4-(2-methylpropyl)phenyl]propanoate (**2**)*

Colorless liquid (CAS: 61566-34-5) [51], yield 95.8%; TLC Rf: 0.81; HPLC t_R (min): 8.34; IR (cm^{-1}): 1740 (C=O, ester).

*Methyl 2-(2-fluoro[1,1′-biphenyl]-4-yl)propanoate (**3**)*

Colorless liquid (CAS: 66202-86-6) [52], yield 65.0%; TLC Rf: 0.78; HPLC t_R (min): 7.98; IR (cm^{-1}): 1733 (C=O, ester).

*Methyl (1,8-diethyl-1,3,4,9-tetrahydropyrano[3,4-b]indol-1-yl)acetate (**4**)*

Yellow solid (CAS: 122188-02-7), yield 76.8%; m.p. 126–127 °C (lit. 128–130 °C) [53], TLC Rf: 0.87; HPLC t_R (min): 11.41; IR (cm^{-1}): 1705 (C=O, ester).

*Methyl 2′,4′-difluoro-4-hydroxy[1,1′-biphenyl]-3-carboxylate (**5**)*

White solid (CAS: 55544-00-8), yield 80.0%; m.p. 92 °C (lit. 95–97 °C) [54]; TLC Rf: 0.89; HPLC t_R (min): 13.59; IR (cm^{-1}): 1702 (C=O, ester).

*Methyl 2-(5-benzoylthiophen-2-yl)propanoate (**6**)*

Yellow liquid (CAS: 32990-41-3), yield 82.0%; TLC Rf: 0.80; HPLC t_R (min): 7.38; IR (cm^{-1}): 1708 (C=O, ester).

*Methyl 3-(4,5-diphenyl-1,3-oxazol-2-yl)propanoate (**7**)*

White solid (CAS: 26820-94-0), yield 77.0%; m.p. 61 °C (lit 56–58 °C) [55]; TLC Rf: 0.85; HPLC t_R (min): 10.70; IR (cm^{-1}): 1735 (C=O, ester).

*Methyl 2-(3-benzoylphenyl)propanoate (**8**)*

Colorless liquid (CAS: 47087-07-0) [56], yield 73%; TLC Rf: 0.82; HPLC t_R (min): 7.90; IR (cm^{-1}): 1734 (C=O, ester), 1657 (C=O, ketone).

*Methyl 2-(6-methoxynaphthalen-2-yl)propanoate (**9**)*

White solid (CAS: 26159-35-3), yield 72.0%; m.p. 82 °C (lit. 88–101 °C) [57]; TLC Rf: 0.84; HPLC t_R (min): 9.59; IR (cm^{-1}): 1740 (C=O, ester).

*Methyl 2-(2,3-dimethylanilino)benzoate (**10**)*

Gray solid (CAS: 1222–42–0), yield 80.0%; m.p. 97–98 °C (lit. 100–102 °C) [58]; TLC Rf: 0.74; HPLC t_R (min): 7.32; IR (cm^{-1}): 1725 (C=O, ester).

*Synthesis of N-[1,3-dihydroxy-2-(hydroxymethyl)propan-2-yl] amide derivatives of selected NSAIDs (**11–20**)*

A mixture of compounds **1**–**10** (10 mmol), tris(hydroxymethyl) aminomethane (TRIS) (10 mmol) and anhydrous K_2CO_3 (10 mmol) in DMSO (10 ml) was heated under reflux at 40–50 °C, for 20 h. When the reaction is over, the mixture was poured into ice water to precipitate the crude product. The crude product, washed with water, was purified by crystallization from a methanol: water mixture, after drying.

*(2S)-2-(3-Benzoylphenyl)-N-[1,3-dihydroxy-2-(hydroxymethyl)propan-2-yl]propanamide (**11**)*

White solid, yield 45.2%; m.p. 56 °C; TLC Rf: 0.56; HPLC t_R (min): 3.08; IR (cm^{-1}): 3549, 3340, 3276 (N–H & O–H), 1666 (C=O, ketone), 1620 (C = O, amide). ^{1}H NMR δ ppm (300 MHz, DMSO-d_6): 1.35 (3H, d, J = *6.9 Hz*, -CHC**H$_3$**), 3.37–3.65 (6H, m, C(C**H$_2$**OH)$_3$ with DMSO peak), 3.82–3.95 (1H, q, C**H**CH$_3$), 4.76 (3H, t, J = *5.7 Hz*, C(CH$_2$O**H**)$_3$), 7.41 (1H, s, -CO***NH***), 7.48–7.80 (9 H, m, Ar-**H**). ^{13}C NMR δ ppm (75 MHz, DMSO-d_6): 18.78 (**C**H$_3$), 44.85 (**C**HCH$_3$), 60.52 (C(**C**H$_2$OH)$_3$), 62.11 (**C**(CH$_2$OH)$_3$), 127.94–142.66 (Ar-**C**), 174.27 (C=O, amide), 195.71 (C=O ketone). MS (EI+) *m/z* calcd for $C_{20}H_{23}NO_5$ $[M + H]^+$ 358.1649, found 358.1636; calcd. for $[M]^{+\cdot}$ 357.1571, found 357.1589; calcd. for $[(M + H)-H_2O]^+$ 340.1543, found 340.1535. Elemental analysis, Calcd. for $C_{20}H_{23}NO_5$.DMSO: C, 60.67; H, 6.71; N, 3.22. Found: C, 60.17; H, 6.24; N, 3.46.

*N-[1,3-Dihydroxy-2-(hydroxymethyl)propan-2-yl]-2-[4-(2-methylpropyl)phenyl]propanamide (**12**)*

White solid, yield 75.8%; m.p. 114 °C; TLC Rf: 0.33; HPLC t_R (min): 2.35; IR (cm^{-1}): 3306 (N–H & O–H), 1630 (C=O). ^{1}H NMR δ ppm (300 MHz, DMSO-d_6): 0.84 (6H, d, J = *6.6 Hz*, CH(C**H$_3$**)$_2$), 1.29 (3H, d, J = *7.2 Hz*, CHC**H$_3$**), 1.68–1.89 (1H, m, C**H**(CH$_3$)$_2$), 2.38 (2H, d, J = *8.7 Hz*, C**H$_2$**CH(CH$_3$)$_2$), 3.48–3.62 (6H, m, C(C**H$_2$**OH)$_3$), 3.67–3.74 (1H, q, C**H**CH$_3$), 4.77 (3H, t, J = *5.5 Hz*, CH(CH$_2$O**H**)$_3$), 7.08 (2H, d, J = *8.1 Hz*, Ar-**H**), 7.20 (1H, s, CON**H**), 7.22 (2H, d, J = *8.0 Hz*, Ar-**H**). ^{13}C NMR δ ppm (75 MHz, DMSO-d_6): 18.78 (CH(**C**H$_3$)$_2$), 22.16 (CH**C**H$_3$), 29.57 (**C**H(CH$_3$)$_2$), 44.21 (**C**H$_2$CH-), 44.78 (**C**HCH$_3$), 60.61 (C(**C**H$_2$OH)$_3$), 62.03 (**C**(CH$_2$OH)$_3$), 125.20–139.39 (Ar-**C**), 174.99 (**C**=O). MS (EI+) *m/z* calcd for $C_{17}H_{27}NO_4$ $[M]^{+\cdot}$ 309.1935, found 309.1916; calcd. for $[M + H]^+$ 310.2013, found 310.2005. Elemental analysis, Calcd. for $C_{17}H_{27}NO_4$: C, 65.99; H, 8.80; N, 4.53. Found: C, 65.82; H, 8.68; N, 4.35.

*N-[1,3-Dihydroxy-2-(hydroxymethyl)propan-2-yl]-2-(2-fluorobiphenyl-4-yl)propanamide (**13**)*

White solid, yield 55.6%; m.p. 173 °C; TLC Rf: 0.29; HPLC t_R (min): 2.27; IR (cm^{-1}): 3312, 3246 (N–H & O–H), 1642 (C=O). ^{1}H NMR δ ppm (300 MHz, DMSO-d_6): 1.35 (3H, d, J = *6.9 Hz*, CH**C**H$_3$), 3.51–3.60 (6H, m, C(C**H$_2$**OH)$_3$), 3.81–3.88 (1H, q, C**H**CH$_3$), 4.75 (3H, t, J = *5.7 Hz and 5.4 Hz*, CH(CH$_2$O**H**)$_3$), 7.24 (1H, s, CON**H**), 7.26–7.58 (8H, m, Ar-**H**). ^{13}C NMR δ ppm (75 MHz, DMSO-d_6): 18.66 (**C**H$_3$), 44.52 (**C**HCH$_3$), 60.53 (C(**C**H$_2$OH)$_3$), 62.17 (**C**(CH$_2$OH)$_3$), 113.37–160.37 (Ar-**C**), 174.11 (**C**=O). MS (EI+) *m/z* calcd for $C_{19}H_{22}FNO_4$ $[M]^{+\cdot}$ 347.1527, found 347.1508; calcd. for $[M + H]^+$ 348.1606, found 348.1597. Elemental analysis, Calcd. for $C_{19}H_{22}FNO_4$: C, 65.69; H, 6.38; N, 4.03. Found: C, 64.78; H, 5.94; N, 4.09.

*N-[1,3-Dihydroxy-2-(hydroxymethyl)propan-2-yl]-2-(1,8-diethyl-1,3,4,9-tetrahydropyrano[3,4-b]indol-1-yl)acetamide (**14**)*

Yellow solid, yield 60.2%; m.p. 164 °C; TLC Rf: 0.38; HPLC t_R (min): 3.75; IR (cm^{-1}): 3393, 3333, 3254 (N–H & O–H), 1628 (C=O). ^{1}H NMR δ ppm (300 MHz, DMSO-d_6): 0.68 (3H, t, J = *7.2 Hz and 7.5 Hz*, CH$_2$C**H$_3$**), 1.25 (3H, t, J = *7.5 Hz*, CH$_2$C**H$_3$**), 1.90–2.06 (2H, m, –C**H$_2$**CH$_3$), 2.49–2.91 (6H, m, –C**H$_2$**CH$_3$ and pyran –C**H$_2$**-), 3.41–3.44 (6H, m, C(C**H$_2$**OH)$_3$), 3.95 (2H, t, J = *5.1 Hz and 5.4 Hz*, -C**H$_2$**CO), 4.84 (3H, t, J = *5.4 Hz and 5.7 Hz*, CH(CH$_2$O**H**)$_3$), 6.86–6.93 (2H, m, Ar-**H**), 7.23 (1H, d, J = *7.2 Hz*, Ar-**H**), 7.28 (1H, s, CON**H**), 10.51 (1H, s, indole –N**H**-). ^{13}C NMR δ ppm (75 MHz, DMSO-d_6): 7.75–30.20 (aliphatic **C**), 44.38, 48.57, 75.55 (heterocyclic **C**), 60.09 (C(**C**H$_2$OH)$_3$), 61.80 (**C**(CH$_2$OH)$_3$), 107.01–135.97 (Ar-**C**), 170.66 (**C**=O). MS (EI+) *m/z* calcd for $C_{21}H_{30}N_2O_5$ $[M]^{+\cdot}$ 390.2149, found 390.2152. Elemental analysis, Calcd. for $C_{21}H_{30}N_2O_5$: C, 64.59; H, 7.74; N, 7.17. Found: C, 64.33; H, 7.86; N, 7.55.

*N-[1,3-Dihydroxy-2-(hydroxymethyl)propan-2-yl]-2′,4′-difluoro-4-hydroxybiphenyl-3-carboxamide (**15**)*

White solid, yield 50%; m.p. 197 °C; TLC Rf: 0.47; HPLC t_R (min): 4.38; IR (cm^{-1}): 3378, 3304, 3202 (N–H & O–H), 1624 (C=O). ^{1}H NMR δ ppm (300 MHz, DMSO-d_6): 3.67 (6H, d, J = *5.4 Hz*, C(C**H$_2$**OH)$_3$), 4.88 (3H, t, J = *5.4 Hz*, CH(CH$_2$O**H**)$_3$), 7.02 1H, d, J = *7.4 Hz*, Ar-**H**), 7.16 (1H, t, J = *7.4 Hz*, Ar-**H**), 7.35 (1H, t, J = *10.2 Hz*, Ar-**H**), 7.51–7.59 (2H, m, Ar-**H**), 8.05 (1H, s, Ar-**H**),

8.57 (1H, s, ArO**H**), 11.85 (1H, s, CON**H**). ^{13}C NMR δ ppm (75 MHz, DMSO-d_6): 60.12 (CH(**C**H_2OH)$_3$), 62.46 (**C**H(CH$_2$OH)$_3$), 104.03–163.03 (Ar-**C**), 166.13 (**C**=O). MS (EI+) *m/z* calcd for $C_{17}H_{17}F_2NO_5$ $[M]^{+\cdot}$ 353.1069, found 353.1079. Elemental analysis, Calcd. for $C_{17}H_{17}F_2NO_5$: C, 57.79; H, 4.85; N, 3.96. Found: C, 58.01; H, 5.03; N, 4.00.

*2-(5-Benzoylthiophen-2-yl)-N-[1,3-dihydroxy-2-(hydroxymethyl)propan-2-yl]propanamide (**16**)*

Yellow solid, yield 43%; m.p. 140–141.5 °C; TLC Rf: 0.39; HPLC t_R (min): 2.86; IR (cm^{-1}): 3351, 3273 (N–H & O–H), 1642 (C=O, ketone), 1620 (C=O, amide). ^{1}H NMR δ ppm (300 MHz, DMSO-d_6): 1.70 (3H, s, CHC**H$_3$**), 3.48–3.59 (6H, m, C(C**H$_2$**OH)$_3$), 4.86 (3H, t, *J = 5.4 Hz*, CH(CH$_2$O**H**)$_3$), 7.14 (1H, s, CON**H**), 7.20 (1H, d, *J = 3.9 Hz*, thiophene Ar-**H**) 7.54–7.82 (7H, m, C**H**(CH$_3$) & Ar-**H**). ^{13}C NMR δ ppm (75 MHz, DMSO-d_6): 28.61 (**C**H$_3$), 59.85 (CH(**C**H$_2$OH)$_3$), 61.00 (**C**H(CH$_2$OH)$_3$), 75.04 (**C**H), 125.32–159.67 (Ar-**C**), 173.02 (**C**=O, amide), 187.40 (**C**=O, ketone). MS (EI+) *m/z* calcd for $C_{18}H_{21}NO_5S$, $[M\text{-}H_2]^+$ 361.0978, found 361.0993. Elemental analysis, Calcd. for $C_{18}H_{21}NO_5S$: C, 59.49; H, 5.82; N, 3.85; S, 8.82. Found: C, 57.24; H, 5.75; N, 3.63; S, 8.67.

*N-[1,3-Dihydroxy-2-(hydroxymethyl)propan-2-yl]-3-(4,5-diphenyl-1,3-oxazol-2-yl)propanamide (**17**)*

White solid, yield 48%; m.p. 148–149 °C; TLC Rf: 0.41; HPLC t_R (min): 3.41; IR (cm^{-1}): 3295, 3258 (N–H & O–H), 1636 (C=O). ^{1}H NMR δ ppm (300 MHz, DMSO-d_6): 2.71 (2H, t, *J = 7.2 Hz and 7.5 Hz*, CH$_2$C**H$_2$**), 3.05 (2H, t, *J = 7.2 Hz and 7.5 Hz*, CH$_2$C**H$_2$**), 3.54–3.56 (6H, m, C(C**H$_2$**OH)$_3$), 4.74 (3H, s, CH(CH$_2$O**H**)$_3$), 7.33–7.59 (11H, m, CON**H** & Ar-**H**). ^{13}C NMR δ ppm (75 MHz, DMSO-d_6): 25.06 (**C**H$_2$), 32.30 (**C**H$_2$), 60.46 (CH(**C**H$_2$OH)$_3$), 62.37 (**C**H(CH$_2$OH)$_3$), 126.21–171.82 (Ar-**C**), 174.74 (**C**=O). MS (EI+) *m/z* calcd for $C_{22}H_{24}N_2O_5$ $[M]^{+\cdot}$ 396.1680, found 396.1673. Elemental analysis, Calcd. for $C_{22}H_{24}N_2O_5$: C, 66.65; H, 6.10; N, 7.07. Found: C, 64.69; H, 5.82; N, 6.85.

*2-(3-Benzoylphenyl)-N-[1,3-dihydroxy-2-(hydroxymethyl)propan-2-yl]propanamide (**18**)*

White solid, yield 55%; m.p. 113.4–114 °C; TLC Rf: 0.56; HPLC t_R (min): 3.08; IR (cm^{-1}): 3460, 3212 (N–H & O–H), 1647 (C=O, ketone), 1628 (C=O, amide). ^{1}H NMR δ ppm (300 MHz, DMSO-d_6): 1.34 (3H, d, *J = 6.9 Hz*, CH(C**H$_3$**)), 3.46–3.57 (6H, m, C(C**H$_2$**OH)$_3$), 3.85–3.92 (1H, q, C**H**(CH$_3$)), 4.70 (3H, t, *J = 5.7 Hz*, CH(CH$_2$O**H**)$_3$), 7.36 (1H, s, CON**H**), 7.48–7.71 (9H, m, Ar-**H**). ^{13}C NMR δ ppm (75 MHz, DMSO-d_6): 18.78 (**C**H$_3$), 44.86 (**C**H), 60.52 (CH(**C**H$_2$OH)$_3$), 62.11 (**C**H(CH$_2$OH)$_3$), 127.95–142.66 (Ar-**C**), 174.27 (**C**=O, amide), 195.71 (**C**=O, ketone). MS (EI+) *m/z* calcd for $C_{20}H_{23}NO_5$, $[M + H]^+$ 358.1649, found 358.1661. MS (EI+) *m/z* calcd for $C_{20}H_{23}NO_5$ $[M + H]^+$ 358.1649, found 358.1638; calcd. for $[(M + H)\text{-}H_2O]^+$ 340.1543, found 340.1564. Elemental analysis, Calcd. for $C_{20}H_{23}NO_5$: C, 67.21; H, 6.49; N, 3.92. Found: C, 66.23; H, 6.43; N, 3.89.

*N-[1,3-Dihydroxy-2-(hydroxymethyl)propan-2-yl]-2-(6-methoxynaphthalen-2-yl)propanamide (**19**)*

White solid, yield 59%; m.p. 126 °C (lit. 126–128 °C) [59]; TLC Rf: 0.35; HPLC t_R (min): 2.87; IR (cm^{-1}): 3314, 3233 (N–H & O–H), 1622 (C=O). ^{1}H NMR δ ppm (300 MHz, DMSO-d_6): 1.40 (3H, d, *J = 6.9 Hz*, CH(C**H$_3$**)), 3.47–3.56 (6H, m, C(C**H$_2$**OH)$_3$), 3.86–3.90 (4H, m, C**H**(CH$_3$) & OC**H$_3$**), 4.75 (3H, s, CH(CH$_2$O**H**)$_3$), 7.14 (1H, d, *J = 8.7 Hz*, Ar-**H**), 7.27–7.28 (2H, m, CON**H** & Ar-**H**), 7.46 (1H, d, *J = 8.4 Hz*, Ar-**H**), 7.73–7.79 (3H, m, Ar-**H**). ^{13}C NMR δ ppm (75 MHz, DMSO-d_6): 18.71 (**C**H$_3$), 45.10 (**C**H), 55.10 (O**C**H$_3$), 60.59 (CH(**C**H$_2$OH)$_3$), 62.07 (**C**H(CH$_2$OH)$_3$), 105.64–156.96 (Ar-**C**), 174.88 (**C**=O). MS (EI+) *m/z* calcd for $C_{18}H_{23}NO_5$ $[M]^{+\cdot}$ 333.1571, found 333.1569; calcd for $[M\text{-}H_2O]^{+\cdot}$ 315.1465, found 315.1460. Elemental analysis, Calcd. for $C_{18}H_{23}NO_5$: C, 64.85; H, 6.95; N, 4.20. Found: C, 63.69; H, 6.69; N, 4.18.

*N-[1,3-Dihydroxy-2-(hydroxymethyl)propan-2-yl]-2-[(2,3-dimethylphenyl)amino]benzamide (**20**)*

White solid, yield 47%; m.p. 150 °C; TLC Rf: 0.49; HPLC t_R (min): 4.03; IR (cm^{-1}): 3287, 3214 (N–H & O–H), 1624 (C = O). ^{1}H NMR δ ppm (300 MHz, DMSO-d_6): 2.10 (3H, s, Ar-C**H$_3$**), 2.27 (3H, s, Ar-C**H$_3$**), 3.93 (6H, d, *J = 5.7 Hz*, C(C**H$_2$**OH)$_3$), 4.74 (3H, t, *J = 5.7 Hz and 6.0 Hz*, CH(CH$_2$O**H**)$_3$), 6.73–6.83 (2H, m, Ar-**H**), 6.90–6.94 (1H, m, Ar-**H**), 7.05–7.06 (2H, m, Ar-**H**), 7.24 (1H, t, *J = 7.8 Hz*, 7.35 (1H, s, N**H**), 7.55 (1H, d, *J = 7.8 Hz*, Ar-**H**), 8.89 (1H, s, CON**H**). ^{13}C NMR δ ppm (75 MHz, DMSO-d_6): 13.53 (**C**H$_3$), 20.26 (**C**H$_3$), 60.10 (CH(**C**H$_2$OH)$_3$), 62.59 (**C**H(CH$_2$OH)$_3$), 114.22–145.22 (Ar-**C**), 169.56 (**C**=O). MS (EI+) *m/z* calcd for $C_{19}H_{24}N_2O_4$ $[M]^{+\cdot}$ 344.1731, found 344.1731. Elemental analysis, Calcd. for $C_{19}H_{24}N_2O_4$: C, 66.26; H, 7.02; N, 8.13. Found: C, 66.01; H, 7.04; N, 8.31

4.2. Biological evaluation

4.2.1. In vivo *pharmacological screening*

Animals. Locally bred BALB/c mice of both sexes (30–35 g) were purchased from the animal breeding laboratories of Inonu University (Malatya, Turkey). The animals were fed a standard pellet diet and water ad libitum in a temperature-controlled room. On the day before the treatments, food was withdrawn, but the animals were allowed free access to water. The allocation of animals to different groups was randomized, and the experiments were carried out under blind conditions. Mice used in the present study were cared for in accordance with the directory of the İnönü University Animal Care Unit, which applies the guidelines of the National Institutes of Health on laboratory animal welfare. Procedures involving animals and their care were conducted in conformity with international laws and policies and animal studies accepted by İnönü University Ethical Council [Protocol No: 2014/A-45 (date: 23.05.2014) and 2015/A-46 (date: 25.05.2015)].

For preliminary anti-inflammatory activity screening, all test drugs were administered to mice at doses of 100 mg/kg (body weight) for 4 animals in each group. For analgesic activity screening, all test drugs were administered to mice at doses of 100 mg/kg (body weight) for 5 animals in each group. Test compounds that possessed more than a 20% inhibitory effect in any of the measurement ranges were selected for further evaluation of the activity-dose relationship in two different doses (50 mg/kg and 200 mg/kg) using groups consisting of 5 animals in the anti-inflammatory activity evaluating. At the end of the anti-inflammatory activity study (at 200 mg/kg dose), the animals were sacrificed by ether anesthesia and stomach, liver and kidneys were removed to assay the tissue lipid peroxidation (LPO), glutathione (GSH) and total thiol group (TSH) levels.

Preparation of test samples for bioassay. Test samples, suspended in a mixture of distilled water and 0.5% sodium carboxymethyl cellulose (CMC), were given orally to the animals. The control group animals received the same experimental handling as those of the test groups, except that the drug treatment was replaced with appropriate volumes of the dosing vehicle. Either indomethacin (INDO, 10 mg/kg), flurbiprofen (FLU, 50 mg/kg) or acetylsalicylic acid (ASA, 200 mg/kg) in 0.5% CMC were used as reference drugs.

Anti-inflammatory activity, carrageenan-induced oedema. For the determination of the effects on carrageenan-induced paw oedema, the modified method of Kasahara et al. was employed [24]. One hour after the oral administration of either test sample or dosing vehicle, each mouse was injected with a freshly prepared (0.5 mg/25 µl) suspension of carrageenan (Sigma, St. Louis, Missouri, U.S.A.) in physiological saline (154 mM NaCl). The subplantar tissue of the right hind paw was the injection site for all mice.

As the control, 25 µl saline solution was injected into the left hind paw. Paw oedema was measured every 90 min for 6 h after induction of inflammation. The difference in footpad thickness between the right and left foot was measured with a pair of dial thickness gauge callipers (Ozaki Co., Tokyo, Japan). Mean values of treated groups were compared with mean values of a control group and analyzed using statistical methods. Percent inhibitory effects were estimated according to the following equation, where n was the average difference in thickness between the left and right hind paw of the control group and n′ was that of the test group of animals.

$$\text{Anti} - \text{inflammatory activity}\ (\%) = [(n - n\prime)/n] \times 100$$

Indomethacin and flurbiprofen were used as reference drugs, administered at 10 mg/kg and 50 mg/kg respectively.

Analgesic activity. One hour after the oral administration of test samples at the dose of 100 mg/kg, each mouse was injected with 3% (w/v) acetic acid solution (0.1 ml/10 g body weight) intraperitoneally. Starting 5 min after the acetic acid injection, the number of muscular contractions on mice was counted for a period of 10 min. A significant reduction in the number of writings by any treatment as compared to control animals was considered as a positive analgesic response. The antinociceptive activity was expressed as percentage change from writhing controls. Percent inhibitory effects were estimated according to the following equation, where n was the average difference in thickness between the left and right hind paw of the control group and n' was that of the test group of animals [60].

$$I\text{nhibition}\,\% = n - n'/n \times 100$$

Lipid peroxidation in tissues. The method was based on the formation of a red chromophore which absorbed at 532 nm, following the reaction of thiobarbituric acid (TBA) with malondialdehyde (MDA) and other breakdown products of peroxidized lipids. Results were expressed as TBARS (nmol/g wet weight tissue) [61,62].

Determination of non protein thiol group (NP-SH, GSH) levels. Non-protein thiol group (NP-SH, GSH) levels were determined according to the methods employed by Sedlak and Lindsay [63]. Reduced glutathione (GSH) was used as standard for calibration of the curve. Stock solution was provided at 2.10^{-4} µmol/ml concentration. Standard solutions were prepared at 0.125, 0.25, 0.5, 1.0 and 2.0×10^{-4} µmol/ml concentrations. Results were expressed as µmol/g wet weight.

Determination of total thiol group (T-SH) levels. Total thiol group (T-SH) levels were determined according to the methods employed by Sedlak and Lindsay [63]. Reduced glutathione (GSH) was used as standard for calibration of the curve. Stock solution was provided at 2.10^{-4} µmol/ml concentration. Standard solutions were prepared at 0.125, 0.25, 0.5, 1.0 and 2.0×10^{-4} µmol/ml concentrations. Results were expressed as µmol/g wet weight.

Acute toxicity test. Animals employed in the carrageenan-induced paw oedema experiment were observed for 72 h, and the mortality rate was recorded for each group at the end of the observation period.

Gastric ulceration studies. Only the animals that were administered 200 mg/kg (body weight) of test samples were subjected to this experimental process. Eight hours after the analgesic activity experiment, mice under deep ether anesthesia were killed, and their stomachs were removed. The abdomen of each mouse was opened through great curvature and, using a dissecting microscope, was examined for lesions or bleeding.

4.2.2. In vitro *COX-1 and −2 enzyme inhibition assay*

This kinetic study was performed using an enzyme immunoassay-based 'COX (ovine/human) Inhibitor Screening Assay' kit (#560131, Cayman Chemical, Ann Arbor, MI, USA). The samples and control were dissolved in the DMSO and diluted with the reaction buffer to their final concentrations. Briefly, COX-1 or COX-2 enzyme, heme and tested compound were added to the supplied buffer solution. These solutions were incubated with COX-1 or COX-2 for 10 min at 37 °C. The reaction was initiated by the addition of 10 μL arachidonic acid (2 mM) as substrate. After incubation at 37 °C for 2 min, the enzyme catalysis was stopped by addition of 30 μL saturated stannous chloride to produce prostaglandin $F_{2\alpha}$ ($PGF_{2\alpha}$) in the presence of prostaglandin H_2 (PGH_2). The tubes were incubated a final time for five minutes at room temperature. The concentration of $PGF_{2\alpha}$ was assayed by ELISA according to the manufacturer's instructions using FLx800 Absorbance Microplate Reader (BioTek Instruments, Inc., Winooski, VT, USA). The results are the means of three single experiments and calculated from a standard curve after the dilution (1/4000). IC_{50} values (required compound concentration causing 50% enzyme inhibition) were determined from six various concentrations via graphic evaluation of the log regression. The selectivity against COX-1 was calculated by dividing the IC_{50} of COX-2 by the IC_{50} of COX-1. The statistical significance of the data was analyzed using Student's *t*-test (GraphPad Prism 6.01, GraphPad Software, Inc. La Jolla, CA, USA).

4.2.3. Mutagenicity studies

Sodium azide (SA), 4-nitro-o-phenylenediamine (NPD), 2-aminofluorene, biotin, histidine, nicotinamide adenine dinucleotide phosphate (NADP), glucose-6-phosphate, ampicillin trihydrate, agar and dimethyl sulfoxide (DMSO) were supplied from Sigma Chemical Company (St Louis, Missouri, USA). Nutrient broth was supplied from HiMedia Laboratories Ltd (Mumbai, Maharashtra, India). The post-mitochondrial fraction (S9) and bacteria were purchased from the Moltox molecular toxicology, Inc (North Carolina, USA).

Ames mutagenicity assay. The tester strains employed were *Salmonella typhimurium* TA98 and TA100 which are primarily recommended by Maron and Ames [64] for routine mutagenicity assays. TA98 detects frameshift and TA100 detects base pair mutagens. Compounds **11, 12** and **13** were dissolved in DMSO and different concentrations up to 5000 µg/plate (1, 10, 100, 1000 and 5000 µg/plate) were used for mutagenicity assay according to OECD guideline [65]. Standard mutagenicity assay in plate incorporation test was carried out both with and without metabolic activation (S9 mix) by following the method of Maron and Ames [64]. Briefly, for each plate to be treated in the absence of metabolic activation, a 2.0 mL of top agar was added to a sterile glass 13 mm culture tube; 0.05 mL aliquot of negative, positive or test chemical solution; and finally, 0.10 mL of the appropriate bacterial culture was added to each tube. To evaluate the impact of test sample metabolites, 0.50 mL of S9 mix was added immediately prior to addition of bacterial culture in the experiment with metabolic activation. The tube contents were immediately vortex mixed then transferred to the surface of the minimal glucose agar plates, inverted and placed at 37 °C for 48 h in dark and revertant colonies were counted after incubation.

Preparation of S9 fraction. The post-mitochondrial fraction (S9) (Aroclor-1254 induced male Sprague Dawley rat liver S9) was used in the preparation of S9-mix as suggested by Maron and Ames [64]. S9 fraction was activated with a combination of NADP and glucose-6-phosphate.

Statistical analysis. In mutagenicity assay, results were expressed as the mean of triplicates ± standard deviation. Dunnett's multiple comparison test was carried out for data in *Salmonella* assay. The value of $p < 0.05$ was considered statistically significant.

4.3. Molecular modeling studies

4.3.1. Preparation of ligands

The synthesized compounds **11**–**20,** co-crystallized inhibitors (2-(1,1′-bifenil-4-il)propanoik asit for COX-1, Celecoxib for COX-2) and reference ligands (Dexketoprofen, (*S)*-Flurbiprofen) were drawn by using the Spartan 04 software [66] (SPARTAN 04, Wavefunction, Inc., Irvine, USA) and optimized for each compound by using the semi-empirical PM3 method. For each compound, the most stable conformation was selected for docking calculation and these pdb files were converted to pdbqt files with The AutoDock Tools program [67].

4.3.2. Preparation of enzymes

The structures of COX-1 (PDB code:1Q4G, resolution:2.0 Å) [68] and COX-2 (PDB code:3LN1, resolution:2.4 Å) [69] were obtained from the protein data bank. The target enzymes were prepared for docking studies using the AutoDock Tools program. Each enzyme was cleaned by removing the water molecules and co-crystallized inhibitors. The charge of the Fe atom in each enzyme was set to +2 manually.

4.3.3. Docking studies

AutoDock Vina software (http://autodock.scripps.edu) was used for all docking experiments [70]. During the docking studies, we used flexible ligand in rigid protein. The Vina parameter "exhaustiveness" was set to the value of 10, besides a grid spacing of 0.375 Å was employed for the calculation of the energetic map of both enzymes. The grid box size was determined as 40 Å × 40 Å × 40 Å and center_x = 26.280, center_y = 33.911, center_z = 202.302 dimensions were used in COX-1 enzyme (1Q4G) docking studies, appropriate to the position of co-crystallized ligand. The size of binding pocket where the celecoxib ligand occupies during crystallization in the 3LN1 structure (COX-2) was accepted as the active site of the enzyme and determined as 40 Å × 40 Å × 40 Å points in x (30.518), y (−21.298), and z (−16.69). To validate the docking protocol, the co-crystallized inhibitors were docked into COX-1 and COX-2 enzymes and the docked pose was in excellent agreement with pdb pose by RMSD values of 0.467 Å and 0.665 Å, respectively.

4.4. In silico *prediction of molecular descriptors, admet and druglikeness profile*

The current study focuses on evaluating solubility and molecular descriptors of compounds **11**–**20**, as well as their ADMET profile. All these compounds were checked for their molecular weight, number of hydrogen bond donors/acceptors, number of rotatable bonds, LogP, solubility, topological polar surface area,%ABS, etc. All of these data were obtained from online webserver SwissADME [44].

ADMET profile such as p-glycoprotein substrate, BBB permeability, AMES toxicity etc. and drug-likeness properties of all synthesized compounds were performed by OSIRIS Datawarrior software [71] besides SwissADME.

Declaration of Competing Interest

The authors declare the following financial interests/personal relationships which may be considered as potential competing interests:

İlkay Kucukguzel reports financial support and equipment, drugs, or supplies were provided by Marmara University, Scientific Research Projects Committee. İlkay Kucukguzel has patent #Synthesis of amide derivatives of some nonsteroidal antiinflammatory drugs as potential pro-drugs (EP2878592A1, 2019) licensed to İlkay Kucukguzel. The authors are grateful to Dr. Jürgen Gross from the Institute of Organic Chemistry, University of Heidelberg, for his generous help on obtaining high resolution mass spectra of the compounds.

One of the co-authors, İrem SET is now working as the Technical Manager MS&T ESO Slovenia at Novartis, since February 2022.

CRediT authorship contribution statement

Necla Kulabaş: Investigation, Methodology, Software, Formal analysis, Visualization, Validation, Writing – original draft, Writing – review & editing. **İrem Set:** Investigation, Methodology, Validation, Formal analysis, Writing – review & editing. **Göknur Aktay:** Methodology, Formal analysis, Writing – original draft, Writing – review & editing. **Şule Gürsoy:** Investigation, Methodology, Formal analysis, Writing – review & editing. **Özkan Danış:** Investigation, Methodology, Formal analysis, Writing – original draft, Writing – review & editing. **Ayşe Ogan:** Methodology, Formal analysis, Writing – original draft, Writing – review & editing. **Safiye Sağ Erdem:** Investigation, Methodology, Software, Visualization, Writing – original draft, Writing – review & editing. **Pınar Erzincan:** Investigation, Software, Formal analysis, Writing – original draft, Writing – review & editing. **Sinem Helvacıoğlu:** Investigation, Methodology, Formal analysis, Writing – review & editing. **Muhammed Hamitoğlu:** Investigation, Methodology, Formal analysis, Writing – original draft, Writing – review & editing. **İlkay Küçükgüzel:** Funding acquisition, Investigation, Methodology, Conceptualization, Supervision, Visualization, Writing – original draft, Writing – review & editing.

Data Availability

The authors are unable or have chosen not to specify which data has been used.

Acknowledgments

This research was supported by Marmara University, Scientific Research Projects Committee; Project Number: SAG-B-080715-0314. The authors are grateful to Dr. Jürgen Gross from the Institute of Organic Chemistry, University of Heidelberg, for his generous help on obtaining high resolution mass spectra of the compounds. Some of the drug substances used in this study were donated as gifts by Abdi İbrahim, Atabay, DEVA and Sanovel Pharmaceutical Companies.

Supplementary materials

Supplementary material associated with this article can be found, in the online version, at doi:10.1016/j.molstruc.2023.135521.

References

[1] P.K. Halen, P.R. Murumkar, R. Giridhar, M.R. Yadav, Prodrug designing of NSAIDs, Mini Rev. Med. Chem. 9 (2009) 124–139, doi:10.2174/138955709787001695.

[2] J. Martel-Pelletier, D. Lajeunesse, P. Reboul, J.P. Pelletier, Therapeutic role of dual inhibitors of 5-LOX and COX, selective and non-selective non-steroidal anti-inflammatory drugs, Ann. Rheum. Dis. 62 (2003) 501–509, doi:10.1136/ard.62.6.501.

[3] G.S. Hassan, S.M. Abou-Seri, G. Kamel, M.M. Ali, Celecoxib analogs bearing benzofuran moiety as cyclooxygenase-2 inhibitors: design, synthesis and evaluation as potential anti-inflammatory agents, Eur. J. Med. Chem. 76 (2014) 482–493, doi:10.1016/j.ejmech.2014.02.033.

[4] B. Balaji, S. Hariharan, D.B. Shah, M. Ramanathan, Discovery of potential and selective COX-1 inhibitory leads using pharmacophore modelling, in silico screening and in vitro evaluation, Eur. J. Med. Chem. 86 (2014) 469–480, doi:10.1016/j.ejmech.2014.09.005.

[5] E.M. Antman, D. DeMets, J. Loscalzo, Cyclooxygenase inhibition and cardiovascular risk, Circulation 112 (2005) 759–770, doi:10.1161/CIRCULATIONAHA.105.568451.

[6] L.A. Perry, C. Mosler, A. Atkins, M. Minehart, Cardiovascular risk associated with NSAIDs and COX-2 inhibitors, US Pharm. 39 (2014) 35–38.

[7] M. Abdel-Aziz, E.A. Beshr, I.M. Abdel-Rahman, K. Ozadali, O.U. Tan, O.M. Aly, 1-(4-Methoxyphenyl)-5-(3,4,5-trimethoxyphenyl)-1H-1,2,4-triazole-3- carboxamides: synthesis, molecular modeling, evaluation of their anti-inflammatory activity and ulcerogenicity, Eur. J. Med. Chem. 77 (2014) 155–165, doi:10.1016/j.ejmech.2014.03.001.

[8] Y. Dündar, S. Ünlü, E. Banoğlu, A. Entrena, G. Costantino, M.T. Nunez, F. Ledo, M.F. Şahin, N. Noyanalpan, Synthesis and biological evaluation of 4,5-diphenyloxazolone derivatives on route towards selective COX-2 inhibitors, Eur. J. Med. Chem. 44 (2009) 1830–1837, doi:10.1016/j.ejmech.2008.10.039.

[9] J.-M. Dogne, C.T. Supuran, D. Pratico, Adverse cardiovascular effects of the coxibs, J. Med. Chem. 48 (2005) 2251–2257.

[10] G.A. Piazza, A.B. Keeton, H.N. Tinsley, J.D. Whitt, B. Gary, B. Mathew, R. Singh, W.E. Grizzle, R.C. Reynolds, NSAIDs: old drugs reveal new anticancer targets, Pharmaceuticals 3 (2010) 1652–1667, doi:10.3390/ph3051652.

[11] M. Madhukar, S. Sawraj, P.D. Sharma, Design, synthesis and evaluation of mutual prodrug of 4-biphenylacetic acid and quercetin tetramethyl ether (BPA-QTME) as gastrosparing NSAID, Eur. J. Med. Chem. 45 (2010) 2591–2596, doi:10.1016/j.ejmech.2010.02.047.

[12] A. Zarghi, S. Arfaei, Selective COX-2 inhibitors: a review of their structure-activity relationships, Iran. J. Pharm. Res. IJPR. 10 (2011) 655–683 http://www.pubmedcentral.nih.gov/articlerender.fcgi?artid=3813081&tool=pmcentrez&rendertype=abstract.

[13] M. Nivsarkar, A. Banerjee, H. Padh, Cyclooxygenase inhibitors: a novel direction for Alzheimer's management, Pharmacol. Rep. 60 (2008) 692–698.

[14] L. Basile, S. Alvarez, A. Blanco, A. Santagati, G. Granata, P. Di Pietro, S. Guccione, M.Á. Muñoz-Fernández, Sulfonilamidothiopyrimidone and thiopyrimidone derivatives as selective COX-2 inhibitors: synthesis, biological evaluation, and docking studies, Eur. J. Med. Chem. 57 (2012) 149–161, doi:10.1016/j.ejmech.2012.09.005.

[15] C. Charlier, C. Michaux, Dual inhibition of cyclooxygenase-2 (COX-2) and 5-lipoxygenase (5-LOX) as a new strategy to provide safer non-steroidal anti-inflammatory drugs, Eur. J. Med. Chem. 38 (2003) 645–659.

[16] S.K. Sharma, C. Karthikeyan, N.S. Hari Narayana Moorthy, D.K. Jain, P. Trivedi, Synthesis and evaluation of some amino acid conjugates of suprofen, Biomed. Prev. Nutr. 3 (2013) 267–272, doi:10.1016/j.bionut.2012.10.015.

[17] P. Yadav, P. Singh, A.K. Tewari, Design, synthesis, docking and anti-inflammatory evaluation of novel series of benzofuran based prodrugs, Bioorganic Med. Chem. Lett. 24 (2014) 2251–2255, doi:10.1016/j.bmcl.2014.03.087.

[18] G.H. Hegazy, H.I. Ali, Design, synthesis, biological evaluation, and comparative Cox1 and Cox2 docking of p-substituted benzylidenamino phenyl esters of ibuprofenic and mefenamic acids, Bioorganic Med. Chem. 20 (2012) 1259–1270, doi:10.1016/j.bmc.2011.12.030.

[19] M.R. Yadav, D.M. Nimekar, A. Ananthakrishnan, P.S. Brahmkshatriya, S.T. Shirude, R. Giridhar, A. Parmar, R. Balaraman, Synthesis of new chemical entities from paracetamol and NSAIDs with improved pharmacodynamic profile, Bioorganic Med. Chem. 14 (2006) 8701–8706, doi:10.1016/j.bmc.2006.08.017.

[20] P.K. Haien, K.K. Chagti, R. Giridhar, M.R. Yadav, Substituted aminoalcohol ester analogs of indomethacin with reduced toxic effects, Med. Chem. Res. 16 (2007) 101–111, doi:10.1007/s00044-007-9013-z.

[21] G.R. Halen PK, M.R. Yadav, K.K. Chagti, C.S. Reshmi, Synthesis and evaluation of dual acting esters of aspirin and ketorolac, Arch. Pharm. (Weinheim). 47 (2006) 61–79.

[22] İ. Küçükgüzel, N. Kulabaş, İ. Set, Synthesis of amdie derivatives of some nonsteroidal antiinflammatory drugs as potential pro-drugs., EP2878592A1, 2019.

[23] S.J. Cho, C. Cui, J.Y. Lee, J.K. Park, S.B. Suh, J. Park, B.H. Kim, K.S. Kim, N-protonation vs O-protonation in strained amides : ab initio study, J. Org. Chem. 62 (1997) 4068–4071, doi:10.1021/jo962063z.

[24] Y. Kasahara, H. Hikino, S. Tsurufuji, M. Watanabe, K. Ohuchi, Antiinflammatory actions of ephedrines in acute inflammations, Planta Med. 4 (1985) 325–331, doi:10.1055/s-2007-969503.

[25] M.P. Holsapple, M. Schnur, G.K.W. Yim, Pharmacological modulation of edema mediated by prostaglandin, serotonin and histamine, Agents Actions 10 (1980) 368–373, doi:10.1007/BF01971442.

[26] A.A. Boligon, R.B. de Freitas, T.F. de Brum, E.P. Waczuk, C.V. Klimaczewski, D.S. de Ávila, M.L. Athayde, L. de Freitas Bauermann, Antiulcerogenic activity of Scutia buxifolia on gastric ulcers induced by ethanol in rats, Acta Pharm. Sin. B. 4 (2014) 358–367, doi:10.1016/j.apsb.2014.05.001.

[27] W.J. Tsai, Y.J. Shiao, S.J. Lin, W.F. Chiou, L.C. Lin, T.H. Yang, C.M. Teng, T.S. Wu, L.M. Yang, Selective COX-2 inhibitors. Part 1: synthesis and biological evaluation of phenylazobenzenesulfonamides, Bioorganic Med. Chem. Lett. 16 (2006) 4440–4443, doi:10.1016/j.bmcl.2006.06.036.

[28] M.A.A. El-Sayed, N.I. Abdel-Aziz, A.A.M. Abdel-Aziz, A.S. El-Azab, Y.A. Asiri, K.E.H. Eltahir, Design, synthesis, and biological evaluation of substituted hydrazone and pyrazole derivatives as selective COX-2 inhibitors: molecular docking study, Bioorganic Med. Chem. 19 (2011) 3416–3424, doi:10.1016/j.bmc.2011.04.027.

[29] I.A. Al-Suwaidan, A.M. Alanazi, A.S. El-Azab, A.M. Al-Obaid, K.E.H. Eltahir, A.R. Maarouf, M.A. Abu El-Enin, A.A.M. Abdel-Aziz, Molecular design, synthesis and biological evaluation of cyclic imides bearing benzenesulfonamide fragment as potential COX-2 inhibitors. Part 2, Bioorganic Med. Chem. Lett. 23 (2013) 2601–2605, doi:10.1016/j.bmcl.2013.02.107.

[30] P. Singh, P. Prasher, P. Dhillon, R. Bhatti, Indole based peptidomimetics as anti-inflammatory and anti-hyperalgesic agents: dual inhibition of 5-LOX and COX-2 enzymes, Eur. J. Med. Chem. 97 (2015) 104–123, doi:10.1016/j.ejmech.2015.04.044.

[31] M. Migliore, D. Habrant, O. Sasso, C. Albani, S.M. Bertozzi, A. Armirotti, D. Piomelli, R. Scarpelli, Potent multitarget FAAH-COX inhibitors: design and structure-activity relationship studies, Eur. J. Med. Chem. 109 (2016) 216–237, doi:10.1016/j.ejmech.2015.12.036.

[32] F.A. Ragab, H.I. Heiba, M.G. El-Gazzar, S.M. Abou-Seri, W.A. El-Sabbagh, R.M. El-Hazek, Anti-inflammatory, analgesic and COX-2 inhibitory activity of novel thiadiazoles in irradiated rats, J. Photochem. Photobiol. B Biol. 166 (2017) 285–300, doi:10.1016/j.jphotobiol.2016.12.007.

[33] K. Wu, J. Dou, H. Ghantous, S. Chen, A. Bigger, D. Birnkrant, Current regulatory perspectives on genotoxicity testing for botanical drug product development in the U.S.A, Regul. Toxicol. Pharmacol. 56 (2010) 1–3, doi:10.1016/j.yrtph.2009.09.012.

[34] C.A. Harman, M.V. Turman, K.R. Kozak, L.J. Marnett, W.L. Smith, R.M. Garavito, Structural basis of enantioselective inhibition of cyclooxygenase-1 by S-α-substituted indomethacin ethanolamides, J. Biol. Chem. 282 (2007) 28096–28105, doi:10.1074/jbc.M701335200.

[35] D.A. Al-Turki, L.A. Abou-Zeid, L.A. Shehata, M.A. Al-Omar, Therapeutic and toxic effects of new NSAIDs and related compounds a review and prospective study, Int. J. Pharmacol. 6 (2010) 813–825.

[36] J.P. Cerón-Carrasco, When virtual screening yields inactive drugs: dealing with false theoretical friends, ChemMedChem 17 (2022) 13–19, doi:10.1002/cmdc.202200278.

[37] K. Yelekçi, S. Sağ Erdem, Computational chemistry and molecular modeling of reversible MAO inhibitors, içinde: claudia Binda (Ed.), Monoamine Oxidase Methods Protoc, Methods Mol. Biol. (2023) 221–252 ss, doi:10.31826/9781463223557-018.

[38] S. Zhong, K. Huang, S. Luo, S. Dong, L. Duan, Improving the performance of the MM/PBSA and MM/GBSA methods in recognizing the native structure of the Bcl-2 family using the interaction entropy method, Phys. Chem. Chem. Phys. 22 (2020) 4240–4251, doi:10.1039/c9cp06459a.

[39] Y. Yuan, J. Pei, L. Lai, LigBuilder V3: a multi-target de novo drug design approach, Front. Chem. 8 (2020) 1083–1091, doi:10.3389/fchem.2020.00142.

[40] Y. Yuan, J. Pei, L. Lai, Binding site detection and druggability prediction of protein targets for structure- based drug design, Curr. Pharm. Des. 19 (2013) 2326–2333, doi:10.2174/1381612811319120019.

[41] Y. Xu, S. Wang, Q. Hu, S. Gao, X. Ma, W. Zhang, Y. Shen, F. Chen, L. Lai, J. Pei, CavityPlus: a web server for protein cavity detection with pharmacophore modelling, allosteric site identification and covalent ligand binding ability prediction, Nucleic Acids Res. 46 (2018) W374–W379, doi:10.1093/nar/gky380.

[42] Ş.G. Küçükgüzel, D. Koç, P. Çikla-Süzgün, D. Özsavci, Ö. Bingöl-Özakpinar, P. Mega-Tiber, O. Orun, P. Erzincan, S. Sarı-Erdem, F. Şahin, Synthesis of tolmetin hydrazide-hydrazones and discovery of a potent apoptosis inducer in colon cancer cells, Arch. Pharm. (Weinheim). 348 (2015) 730–742, doi:10.1002/ardp.201500178.

[43] P. Tziona, P. Theodosis-Nobelos, G. Papagiouvannis, A. Petrou, C. Drouza, E.A. Rekka, Enhancement of the anti-inflammatory activity of NSAIDs by their conjugation with 3,4,5-trimethoxybenzyl alcohol, Molecules 27 (2022) 1–18, doi:10.3390/molecules27072104.

[44] A. Daina, O. Michielin, V. Zoete, SwissADME: a free web tool to evaluate pharmacokinetics, drug-likeness and medicinal chemistry friendliness of small molecules, Sci. Rep. 7 (2017) 1–13, doi:10.1038/srep42717.

[45] C.A. Lipinski, F. Lombardo, B.W. Dominy, P.J. Feeney, Experimental and computational approaches to estimate solubility and permeability in drug discovery and development settings, Adv. Drug Deliv. Rev. 23 (1997) 3–25.

[46] A.K. Ghose, V.N. Viswanadhan, J.J. Wendoloski, A knowledge-based approach in designing combinatorial or medicinal chemistry libraries for drug discovery. 1. A qualitative and quantitative characterization of known drug databases, J. Comb. Chem. 1 (1999) 55–68.

[47] D.F. Veber, S.R. Johnson, H.Y. Cheng, B.R. Smith, K.W. Ward, K.D. Kopple, Molecular properties that influence the oral bioavailability of drug candidates, J. Med. Chem. 45 (2002) 2615–2623, doi:10.1021/jm020017n.

[48] I. Muegge, S.L. Heald, D. Brittelli, Simple selection criteria for drug-like chemical matter, J. Med. Chem. 44 (2001) 1841–1846.

[49] Y.H. Zhao, M.H. Abraham, J. Le, A. Hersey, C.N. Luscombe, G. Beck, B. Sherborne, I. Cooper, Rate-limited steps of human oral absorption and QSAR studies, Pharm. Res. 19 (2002) 1446–1457, doi:10.1023/A:1020444330011.

[50] Ş.G. Küçükgüzel, A. Mazi, F. Şahin, S. Öztürk, J. Stables, Synthesis and biological activities of diflunisal hydrazide-hydrazoness, Eur. J. Med. Chem. 38 (2003) 1005–1013, doi:10.1016/j.ejmech.2003.08.004.

[51] D.V. Patil, M.S. Wadia, A novel approach to the synthesis of 2-aryl propionates, Synth. Commun. 32 (2002) 2821–2827, doi:10.1081/SCC-120006466.

[52] S. Aydin, N. Kaushik-Basu, P. Arora, A. Basu, D.B. Nichols, T.T. Talele, M. Akkurt, I. Çelik, O. Büyükgungör, Ş.G. Kucukguzel, Microwave assisted synthesis of some novel flurbiprofen hydrazidehydrazones as anti-HCV NS5B and anticancer agents, Marmara Pharm. J. 17 (2013) 26–34, doi:10.12991/201317389.

[53] P. Çikla, D. Özsavci, Ö. Bingöl-Özakpinar, A. Şener, Ö. Çevik, S. Özbaş-Turan, J. Akbuğa, F. Şahin, Ş.G. Küçükgüzel, Synthesis, cytotoxicity, and pro-apoptosis

activity of etodolac hydrazide derivatives as anticancer agents, Arch. Pharm. (Weinheim) 346 (2013) 367–379, doi:10.1002/ardp.201200449.
[54] H.D. Tabba, M.E. Abdel-Hamid, M.S. Suleiman, M.M. Al-Arab, M.M. Hasan, S. Abu-Lafi, N.M. Najib, Synthesis, identification and preliminary evaluation of esters and amide derivatives of diflunisal, Int. J. Pharm. 54 (1989) 57–63, doi:10.1016/0378-5173(89)90165-8.
[55] P. Rayam, N. Polkam, N. Kuntala, V. Banothu, H.S. Anantaraju, Y. Perumal, S. Balasubramanian, J.S. Anireddy, Design and synthesis of oxaprozin-1,3,4-oxadiazole hybrids as potential anticancer and antibacterial agents, J. Heterocycl. Chem. 57 (2020) 1071–1082, doi:10.1002/jhet.3842.
[56] H. Neumann, A. Brennführer, M. Beller, An efficient and practical sequential one-pot synthesis of suprofen, ketoprofen and other 2-arylpropionic acids, Adv. Synth. Catal. 350 (2008) 2437–2442, doi:10.1002/adsc.200800415.
[57] I.T. Harrison, B. Lewis, P. Nelson, W. Rooks, A. Roszkowski, A. Tomolonis, J.H. Fried, Nonsteroidal antiinflammatory agents. I. 6-Substituted 2-naphthylacetic acids, J. Med. Chem. 13 (1970) 203–205.
[58] H. Lgaz, A. Chaouiki, M.R. Albayati, R. Salghi, Y. El Aoufir, I.H. Ali, M.I. Khan, S.K. Mohamed, I.M. Chung, Synthesis and evaluation of some new hydrazones as corrosion inhibitors for mild steel in acidic media, Res. Chem. Intermed. 45 (2019) 2269–2286, doi:10.1007/s11164-018-03730-y.
[59] R.K. Das, S. Banerjee, G. Raffy, A. Del Guerzo, J.P. Desvergne, U. Maitra, Spectroscopic, microscopic and first rheological investigations in charge-transfer interaction induced organogels, J. Mater. Chem. 20 (2010) 7227–7235, doi:10.1039/c0jm01192d.
[60] R. Koster, M. Anderson, E.J. DeBeer, Acetic acid for analgesic screening, Fed. Proc. 18 (1959) 412.
[61] H. Ohkawa, N. Ohishi, K. Yagi, Assay for lipid peroxides in animal tissues by thiobarbituric acid reaction, Anal. Biochem. 95 (1979) 351–358, doi:10.1016/0003-2697(79)90738-3.
[62] I.S. Jamall, J. Crispin Smith, Effects of cadmium on glutathione peroxidase, superoxide dismutase, and lipid peroxidation in the rat heart: a possible mechanism of cadmium cardiotoxicity, Toxicol. Appl. Pharmacol. 80 (1985) 33–42, doi:10.1016/0041-008X(85)90098-5.
[63] J. Sedlak, R.H. Lindsay, Estimation of total protein-bound and nonprotein sulfhydryl groups in tissue with Ellman's reagent, Anal. Biochem. 25 (1968) 192–205.
[64] D.M. Maron, B.N. Ames, Revised methods for the Salmonella mutagenicity test, Mutat. Res. Mutagen. Relat. Subj. 113 (1983) 173–215, doi:10.1016/0165-1161(83)90010-9.
[65] OECD Guideline for Testing of Chemicals: Bacterial Reverse Mutation Test., içinde: OECD Publishing, Paris, 1997: s. TG 471.
[66] J.J.P. Stewart, Optimization of parameters for semiempirical methods V: modification of NDDO approximations and application to 70 elements, J. Mol. Model. 13 (2007) 1173–1213, doi:10.1007/s00894-007-0233-4.
[67] G.M. Morris, R. Huey, W. Lindstrom, M.F. Sanner, R.K. Belew, D.S. Goodsell, A.J. Olson, Software news and updates gabedit — a graphical user interface for computational chemistry softwares, J. Comput. Chem. 30 (2009) 174–182, doi:10.1002/jcc.
[68] K. Gupta, B.S. Selinsky, C.J. Kaub, A.K. Katz, P.J. Loll, The 2.0 Å resolution crystal structure of prostaglandin H2 synthase-1: structural insights into an unusual peroxidase, J. Mol. Biol. 335 (2004) 503–518, doi:10.1016/J.JMB.2003.10.073.
[69] J.L. Wang, D. Limburg, M.J. Graneto, J. Springer, J.R.B. Hamper, S. Liao, J.L. Pawlitz, R.G. Kurumbail, T. Maziasz, J.J. Talley, J.R. Kiefer, J. Carter, The novel benzopyran class of selective cyclooxygenase-2 inhibitors. Part 2: the second clinical candidate having a shorter and favorable human half-life, Bioorg. Med. Chem. Lett. 20 (2010) 7159–7163, doi:10.1016/J.BMCL.2010.07.054.
[70] T. Oleg, O.A. J, AutoDock Vina: improving the speed and accuracy of docking with a new scoring function, efficient optimization, and multithreading, J. Comput. Chem. 31 (2010) 455–461, doi:10.1002/jcc.21334.
[71] T. Sander, J. Freyss, M. Von Korff, C. Rufener, DataWarrior: an open-source program for chemistry aware data visualization and analysis, J. Chem. Inf. Model. 55 (2015) 460–473, doi:10.1021/ci500588j.